

**The impacts of drought on water availability
spatial and temporal analysis in the Belt and Road region (2001–2020)**

Lu, Jing; Jia, Li; Menenti, Massimo; Zheng, Chaolei; Hu, Guangcheng; Ji, Dabin

DOI

[10.1080/17538947.2025.2449706](https://doi.org/10.1080/17538947.2025.2449706)

Publication date

2025

Document Version

Final published version

Published in

International Journal of Digital Earth

Citation (APA)

Lu, J., Jia, L., Menenti, M., Zheng, C., Hu, G., & Ji, D. (2025). The impacts of drought on water availability: spatial and temporal analysis in the Belt and Road region (2001–2020). *International Journal of Digital Earth*, 18(1), Article 2449706. <https://doi.org/10.1080/17538947.2025.2449706>

Important note

To cite this publication, please use the final published version (if applicable).
Please check the document version above.

Copyright

Other than for strictly personal use, it is not permitted to download, forward or distribute the text or part of it, without the consent of the author(s) and/or copyright holder(s), unless the work is under an open content license such as Creative Commons.

Takedown policy

Please contact us and provide details if you believe this document breaches copyrights.
We will remove access to the work immediately and investigate your claim.



The impacts of drought on water availability: spatial and temporal analysis in the Belt and Road region (2001–2020)

Jing Lu, Li Jia, Massimo Menenti, Chaolei Zheng, Guangcheng Hu & Dabin Ji

To cite this article: Jing Lu, Li Jia, Massimo Menenti, Chaolei Zheng, Guangcheng Hu & Dabin Ji (2025) The impacts of drought on water availability: spatial and temporal analysis in the Belt and Road region (2001–2020), International Journal of Digital Earth, 18:1, 2449706, DOI: [10.1080/17538947.2025.2449706](https://doi.org/10.1080/17538947.2025.2449706)

To link to this article: <https://doi.org/10.1080/17538947.2025.2449706>



© 2025 The Author(s). Published by Informa UK Limited, trading as Taylor & Francis Group



Published online: 08 Jan 2025.



Submit your article to this journal [↗](#)



Article views: 221







View related articles [↗](#)



View Crossmark data [↗](#)

The impacts of drought on water availability: spatial and temporal analysis in the Belt and Road region (2001–2020)

Jing Lu ^a, Li Jia ^{a,b}, Massimo Menenti ^{a,c}, Chaolei Zheng ^a, Guangcheng Hu ^a and Dabin Ji ^a

^aKey Laboratory of Remote Sensing and Digital Earth, Aerospace Information Research Institute, Chinese Academy of Sciences, Beijing, People's Republic of China; ^bInternational Research Center of Big Data for Sustainable Development Goals, Aerospace Information Research Institute, Chinese Academy of Sciences, Beijing, People's Republic of China; ^cFaculty of Civil Engineering and Geosciences, Delft University of Technology, Delft, The Netherlands

ABSTRACT

Climate change, population growth, and economic development exacerbate water scarcity. This study investigates the impact of drought on water availability in the Belt and Road region using high-resolution remote sensing data from 2001 to 2020. The results revealed an average water availability (precipitation minus evapotranspiration) of 249 mm/year and a declining trend in the Belt and Road region. Approximately 13% of the Belt and Road region faces water deficits (evapotranspiration exceeds precipitation), primarily in arid and semi-arid regions with high drought frequency. The area in the water deficit is expanding, and the intensity of the water deficit is increasing. The annual trend of water availability is strongly related to the frequency of droughts, i.e. water availability decreases with increased drought frequency. Drought exacerbates seasonal water stress in approximately one-third of the Belt and Road region, mainly in Europe and northern Asia, where drought frequently occurs during seasons with low water availability. The more severe the drought, the larger the negative anomaly in water availability. The critical role of evapotranspiration in seasonal water availability variability is also highlighted. This research underscores the importance of understanding drought-induced changes in water availability, which is crucial for sustainable water resource management.

ARTICLE HISTORY

Received 2 July 2024




Accepted 31 December 2024

KEYWORDS

Water availability; drought; spatial and temporal characteristics; the Belt and Road region

1. Introduction

Water is crucial for human well-being and sustainable global development (Sjöstrand 2023; UNESCO 2021). Climate warming is accelerating the global water cycle with increasing precipitation and evapotranspiration in some regions and exacerbating dryland conditions and droughts in other places (Schlaepfer et al. 2017; Huang et al. 2016; Zhang et al. 2023; Chen and Wang 2022; Yuan et al. 2023). These changing conditions, in turn, result in insufficient water supply (Qiu, Shen, and Xie 2023). Population growth and economic development also increase the conflict between water demand and supply (He et al. 2021; WMO 2022). Water availability, defined as the balance

CONTACT Jing Lu  jjali@aircas.ac.cn; Li Jia  jjali@aircas.ac.cn  Key Laboratory of Remote Sensing and Digital Earth, Aerospace Information Research Institute, Chinese Academy of Sciences, Beijing, 100101, People's Republic of China

© 2025 The Author(s). Published by Informa UK Limited, trading as Taylor & Francis Group

This is an Open Access article distributed under the terms of the Creative Commons Attribution-NonCommercial License (<http://creativecommons.org/licenses/by-nc/4.0/>), which permits unrestricted non-commercial use, distribution, and reproduction in any medium, provided the original work is properly cited. The terms on which this article has been published allow the posting of the Accepted Manuscript in a repository by the author(s) or with their consent.

between water inputs and outputs, namely precipitation (P) minus evapotranspiration (ET) (P-ET) (Byrne and O’Gorman 2015; Khorrami and Gündüz 2023), is a critical aspect of the water cycle. This balance represents the total water available for runoff, soil water storage changes, and groundwater recharge (Kumar et al. 2014). Changes in water availability are significant for freshwater supply, food security, and the sustainability of natural ecosystems, particularly in water-limited ecosystems, where vegetation growth largely depends on water availability (Zhao, Ma, and Wu 2021; Zhou et al. 2021). Therefore, understanding and addressing water availability, especially in dry conditions, is essential for sustainable development.

Researchers have conducted extensive assessments of global water availability. Padrón et al. (2020) employed data-driven and land-surface models to reconstruct global P-ET from 1902 to 2014, revealing changes in water availability during the dry season. Zhang et al. (2023) utilized P-ET data from an ensemble of multi-source data to quantify the global land water availability trend from 2001 to 2020. Liu et al. (2018) calculated P-ET using outputs from atmospheric general circulation models to assess changes in water availability below normal conditions in the +1.5°C and +2°C warming scenarios. P-ET, representing net water flux, was utilized to evaluate the down-scaled potentially available water storage index, revealing local water stress conditions (Khorrami 2023). These studies highlight how climate change significantly affects the timing and intensity of precipitation and evapotranspiration, resulting in shifts in water availability. Seasonal water availability patterns can be altered by changes in precipitation timing, rising temperatures, solar irradiance, and wind speed (Hajek and Knapp 2022). These factors influence evapotranspiration and water availability independently of precipitation changes (Konapala et al. 2020). These studies significantly enhance our understanding of global water availability dynamics and the complex interplay between climate variables, thereby aiding in mitigating the impacts of climate change on water resources.

The multi-annual P-ET is generally positive and balanced by runoff over a large spatial scale, but this balance does not always hold on seasonal or local scales (Chou et al. 2013; Kumar et al. 2015). Positive P-ET values indicate a water surplus where precipitation exceeds evapotranspiration, increasing water storage. Conversely, negative P-ET values denote a water deficit, where evapotranspiration exceeds precipitation, necessitating the utilization of groundwater and external water resources to meet the demand, implying low water availability or water scarcity (Condon, Atchley, and Maxwell 2020; Giardina et al. 2023). Current research often overlooks the seasonal variability in water availability, focusing typically on annual averages, which can mask critical seasonal differences. Allan (2023) analyzed annual maximum and minimum P-ET values and their changes globally over land and ocean using observation-based datasets and CMIP6 climate model experiments spanning 1950–2100, concluding that an amplified seasonal range in P-ET is to be expected. In arid and semi-arid regions, the seasonal timing of water availability is crucial for vegetation status, ecosystem sustainability, and carbon cycles (Gudmundsson, Greve, and Seneviratne 2016; Murray-Tortarolo et al. 2016). However, current studies on the seasonal characteristics of water availability are still inadequate, particularly in water-limited regions. In addition, areas with negative P-ET values are difficult to identify due to the coarse spatial resolution of data used in previous studies.

Drought is a complex, naturally occurring hazard related to climate variability and change. Drought occurs due to deviations from normal patterns in precipitation and temperature, resulting in severe impacts on agriculture, forestry, the environment, and water supply (Abrar Faiz et al. 2022; AghaKouchak et al. 2015; Kang et al. 2024). Drought is a natural hazard characterized by a water deficit, but it emphasizes the anomaly below normal water conditions. Droughts can occur in any region, and different ecosystems exhibit significant variations in their responses to drought (Li et al. 2021; Zhao et al. 2016). Water availability, expressed as P-ET, is closely related to renewable water resources (Lu et al. 2019). High P-ET values indicate more water resources, while low or negative P-ET values denoting water deficits indicate water scarcity or dry conditions, different from droughts. During drought periods, evapotranspiration frequently increases (Zhao et al. 2022), leading to water availability change. The impact of drought on water availability may be more severe in

water-limited regions and during dry seasons, increasing water stress. With climate change, global droughts are intensifying and shifting from slow droughts to flash droughts (Rohde 2023; Yuan et al. 2023). How drought impacts the change in water availability remains a topic requiring further research.

The Belt and Road region, from the Belt and Road Initiative, spans Asia, Africa, Europe, and Oceania. Two-thirds of the land in this region is categorized as arid or semi-arid. The distribution of water resources along the Belt and Road is uneven, resulting in various water-related challenges, such as water scarcity, deforestation, drought, floods, air and water pollution, and habitat degradation (Compagno et al. 2022; Deng and Chen 2017; Dewan 2015; Dube et al. 2023; Hong et al. 2023). Droughts frequently occur in this region, particularly in Southern China, South Asia, and Southeast Asia (Venkatappa et al. 2021). These natural hazards pose significant challenges to global sustainable development (Guo 2018; UN 2023; Zhang et al. 2022). Moreover, the Belt and Road region is home to over two-thirds of the world's population and is a primary cropland area. Water availability is one of the critical challenges in this region, as it is particularly vulnerable to drought due to its water-limited conditions and high population density. Increased efforts have been made in the region to address water resource challenges (Guo et al. 2017; Guo et al. 2018; Jia et al. 2017). A series of water-related datasets with high spatial and temporal resolution has been generated, including precipitation, evapotranspiration, water bodies, soil moisture, and others (Han and Niu 2020; Zheng, Jia, and Hu 2022; Zheng, Jia, and Zhao 2023), providing valuable new data for water-related research.

For a deeper understanding of how droughts impact water availability, this study selects the Belt and Road region as the focal area for analysis. It aims to investigate the relationship between drought characteristics and the spatial-temporal patterns of water availability using high-spatial and temporal resolution remote sensing data with high accuracy for precipitation and evapotranspiration. The water deficit areas, annual trends, seasonality, and anomalies in water availability will be extracted to build the correlation with drought frequency, severity, seasonality, and trends. The study seeks to address the following questions:

- (1) What is the correlation between drought occurrences and water deficits?
- (2) To what extent does drought influence the annual and seasonal trends in water availability?
- (3) Where does drought exacerbate seasonal water stress the most?
- (4) How significant are the drought-induced anomalies in water availability?

This study will provide crucial insights into the effects of droughts on water availability, thereby facilitating the development of effective adaptation strategies to mitigate drought-induced water scarcity.

2. Materials

2.1. Study area

This study focuses on the Belt and Road region, covering Asia, Europe, Africa, and Oceania (Figure 1a). More than three-fourths of the land in this region is located in the Northern Hemisphere. According to Aridity Index values provided by Zomer et al. (2022), the dry areas, including Hyper Arid, Arid, Semi-Arid, and Dry Sub-humid, account for two-thirds of the Belt and Road region. These areas constitute more than half of the same types of areas worldwide. Nearly all Hyper-Arid areas are distributed in this region, and over 80% of the world's Arid areas are located here. Additionally, two-thirds of the world's Semi-Arid and Dry Sub-humid areas are in this region. Moreover, nearly 80% of the world's cropland and more than 80% of its irrigated areas are located in this region (Figure 1b). Therefore, water availability is crucial in this region.

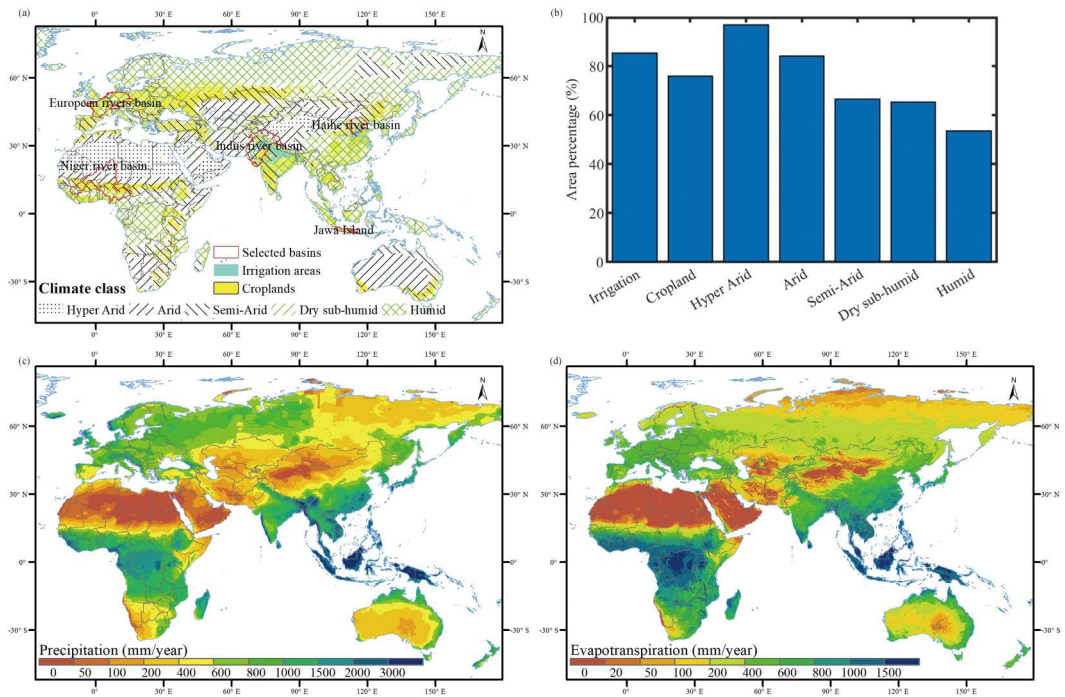


Figure 1. Hydrological and climate characteristics of the Belt and Road region, (a) Agricultural land use and climate types of the Belt and Road region, (b) Fractional abundance of climate types, cropland, and irrigated lands in the study region compared to the world, (c) Multi-year average precipitation, and (d) Multi-year average evapotranspiration.

In addition to analyzing the entire Belt and Road region, this study also focuses on five different river basins. These basins, distributed across different climate regions and continents, are the European rivers basin, the Haihe River basin, the Niger River basin, the Jawa Island rivers basin, and the Indus River basin. The European rivers basin and the Jawa Island rivers basin are located in humid regions, while the other three basins are in arid and semi-arid areas. Basin boundaries are delineated using HydroBASINS level 3 basin units (Lehner and Grill 2013) and are shown in Figure 1a. Each of these five basins has a population exceeding 100 million people, and many cropland and irrigated areas are found within these basins.

Precipitation and evapotranspiration are essential variables for water availability. The spatial distributions of multi-year average P and ET are shown in Figures 1c and d, respectively. ET generally varies with P, with higher values in low-latitude and coastal regions.

2.2. Data

2.2.1. Precipitation

The precipitation data are sourced from the downscaled TRMM-3B42 precipitation fusion product, which has a spatial resolution of 0.25° . By incorporating the infrared band fusion data from a global stationary satellite with high spatial and temporal resolution (NCEP/CPC Half Hourly 4 km Global Merged IR), as well as high-resolution surface elevation and vegetation index data, a matching model between the stationary satellite infrared brightness temperature data and the TRMM-3B42 precipitation fusion data was established. This matching model and a downscaling model were used to generate high-resolution precipitation data at 0.05° every half hour. These high-resolution precipitation data are available through the CASEarth Data Sharing and Service Portal (<https://data.casearth.cn>). Monthly and yearly precipitation were then calculated by aggregating the half-hour data.

The downloaded high-resolution precipitation data at 0.05° is more consistent with GPCP precipitation data than with CHIRPS precipitation data of the same resolution in the Belt and Road region, better than GPM data. The downscaled fusion product covers the area from 50°S to 50°N, following the coverage of the TRMM-3B42 product. Beyond this region, precipitation data from the GPM at 0.1° resolution is used and resampled to 0.05°.

2.2.2. Evapotranspiration

The actual evapotranspiration data was generated using the ETMonitor model. ETMonitor is a remote sensing-based ET model that comprehensively considers the water balance, energy exchange, and vegetation physiological processes. Driven by multi-source remote sensing data and the atmospheric reanalysis data ERA5, the ETMonitor model is suitable for different land cover types and can produce long-term continuous spatiotemporal surface evapotranspiration datasets with higher accuracy and more reasonable spatial patterns compared to other ET products (Zheng et al., 2022). The estimated daily ET was validated based on the global in situ observation across various ecosystems, with an overall high correlation of 0.75 and a low root mean square error of 0.93 mm d⁻¹.

The global daily ET product at 1 km spatial resolution can be downloaded from the CASEarth Data Sharing and Service Portal (https://data.casearth.cn/thematic/GWRD_2023/272). Daily ET data at 1 km resolution were accumulated to monthly and yearly values. To be consistent with the spatial resolution of precipitation data, ET data at 1 km resolution was resampled to 0.05° using the nearest neighbor interpolation method.

2.2.3. Drought index

The scPDSI (self-calibrating Palmer Drought Severity Index) global gridded dataset, downloaded from <https://crudata.uea.ac.uk/cru/data/drought/#global>, is used to identify the characteristics of drought in this study. The temporal and spatial resolution of the scPDSI gridded dataset are monthly and 0.5°, respectively. The CRU high-resolution surface climate dataset (CRU TS 4.07 version) is used as input to calculate the global scPDSI dataset. The potential evapotranspiration (PET) was calculated using the Penman-Monteith method. This more physically based PET method incorporates information on radiation, humidity, wind speed, and vegetation resistance rather than just temperature (van der Schrier, Jones, and Briffa 2013).

The scPDSI has been widely used in the research community for spatiotemporal investigations of drought and numerous studies on the impact of drought on crops, vegetation, and ecosystems (Mondal et al. 2023; Pandžić et al. 2022). Furthermore, scPDSI is a popular indicator for global-scale drought analysis under global warming (Barichivich et al. 2021). As such, scPDSI is a priority indicator of the relative extent, spatial location, and severity of drought.

2.2.4. Aridity index

Aridity is usually expressed as a generalized function of precipitation, temperature, and reference evapotranspiration. An Aridity Index (AI) can be used to quantify precipitation availability over atmospheric water demand. The AI used in this study is from the Global Aridity Index (Global-AI) datasets in version 3, at 30 arc seconds or approximately 1 km at the equator, which was driven by WorldClim climatic variables (Zomer, Xu, and Trabucco 2022). This data can be downloaded online and is available at https://figshare.com/articles/dataset/Global_Aridity_Index_and_Potential_Evapotranspiration_ET0_Climate_Database_v2/7504448?file=36324084. According to AI values, the generalized climate is classified into five types:

- (1) Hyper Arid (AI < 0.03),
- (2) Arid (0.03 ≤ AI < 0.2),
- (3) Semi-Arid (0.2 ≤ AI < 0.5),
- (4) Dry Sub-humid (0.5 ≤ AI < 0.65), and
- (5) Humid (AI ≥ 0.65).

The climate classification was used to analyze the relationship between water deficit, changes in water availability and aridity.

3. Methods

3.1. Overall framework

The overall framework of this study is depicted in Figure 2, with water availability and drought as the primary focus. P-ET serves as the metric of water availability (WA). Spatial and temporal characteristics of water availability, including areas of water deficit, inter-annual trends, seasonality, and anomalies, were extracted using time series of P-ET. Drought characteristics, encompassing frequency, severity, and seasonality, were extracted based on scPDSI. Methods for extracting drought characteristics and the spatial-temporal patterns of water availability will be detailed in sections 2.2–2.6. Correlation analysis will be employed to establish the relationship between drought and water availability. Additionally, climate types will be classified using the aridity index. All analyses aim to address the four questions mentioned above.

3.2. Trend analysis method

The interannual trend is a critical characteristic of time series data, reflecting the long-term change of variables. Sen’s slope estimator, a non-parametric procedure developed by Sen (1968), was utilized to estimate the trend of water availability. Positive values of Sen’s slope indicate increasing trends, while negative values denote decreasing trends.

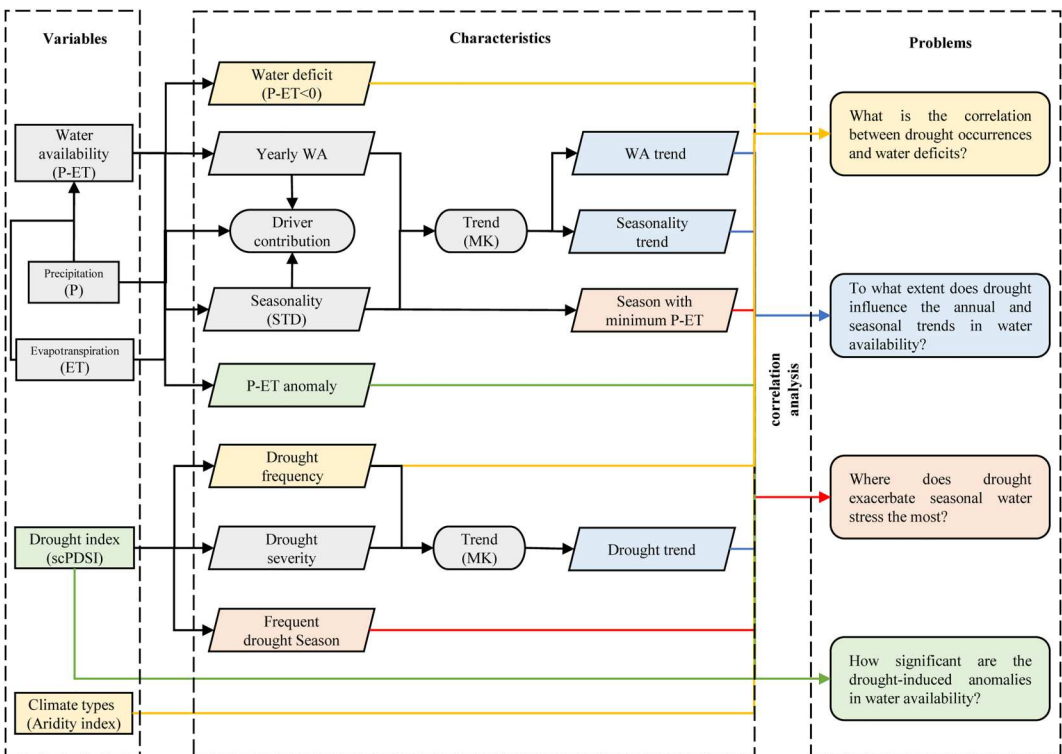


Figure 2. The overall framework of this work (different colors correspond to the various problems).

The significance of trend is determined using the Mann–Kendall (MK) trend test method, a rank-based non-parametric approach. The MK test quantifies both the magnitude and direction of trends in data and is closely related to Sen’s slope. A larger absolute value of the z-statistic indicates a stronger trend, whether increasing or decreasing, depending on the sign of the statistic. If $|z| > 1.96$, it suggests that the trend is statistically significant at the 95% confidence level, corresponding to a significance level of 0.05. For $|z| > 1.645$, the trend passes a weaker significance test at the 90% confidence level, corresponding to a significance level of 0.1.

In addition to examining the interannual trend of yearly water availability, this study also investigates the seasonality of water availability and its trends. Drought trend characteristics are assessed using the MK method based on annual drought frequency and severity.

3.3. Seasonality calculation

Seasonality reflects the variability within a year. In this study, the standard deviation will be used to calculate P-ET seasonality and the changes in dry and wet conditions throughout the year. The standard deviation is a common measure of statistical dispersion used in probability statistics. It is defined as the square root of the arithmetic mean of the squared differences between the individual values and their mean. It quantifies the degree of dispersion among individuals in a group. The standard deviation (STD) is calculated using the following equation:

$$\text{STD} = \sqrt{\frac{\sum (x_i - \mu)^2}{N}} \quad (1)$$

x_i represents each monthly value in one year. μ represents the mean of the monthly values in 1 year. N is 12 in this study.

A larger standard deviation indicates more significant variability within a year, reflecting a more substantial seasonal effect. Conversely, a smaller standard deviation suggests less seasonal variability. Standard deviation has been widely employed for seasonality analysis of geographical variables (Wang et al. 2024; Wasko, Nathan, and Peel 2020). This study employs standard deviation due to its straightforward application. Additionally, standard deviation allows a straightforward comparison of the seasonality of various variables, such as P, ET, and P-ET, as well as conducting trend analysis of seasonality.

In addition to assessing the seasonality of water availability, the season characterized by the minimum P-ET is also extracted to evaluate its relationship with frequent drought occurrences. Four seasons are divided according to the month. The March to May period is classified as the first season, then June to August, September to November, and December to the next February, corresponding to the Northern hemisphere Spring, Summer, Autumn, and Winter. The season with minimum P-ET indicates low water availability and high water stress. Frequent droughts during periods of low water availability can exacerbate seasonal water stress, leading to a more severe water crisis. Identifying areas where drought exacerbates seasonal water stress is crucial for effective water resources management.

3.4. Drought characteristics identification

Frequency, severity, and timing of occurrence are critical characteristics of droughts, and the selection of a drought index significantly influences the assessment of these parameters. Given the complexity of drought, numerous indices have been developed for monitoring purposes (AghaKouchak et al. 2015). In this study, the scPDSI, a robust drought index introduced by Wells, Goddard, and Hayes (2004), is utilized to identify drought characteristics. The scPDSI is a modified version of the original Palmer Drought Severity Index (PDSI) developed by Palmer (1965), aimed at improving comparability across diverse climate regimes. scPDSI is computed using a time series of

precipitation and temperature data along with fixed parameters that account for soil and surface characteristics specific to each location.

The threshold level method is employed to determine the onset and cessation of drought events. A drought event begins when the drought index drops below a predefined threshold and continues until the threshold is surpassed. Different thresholds correspond to varying degrees of drought severity. Following the methodology established by Wells, Goddard, and Hayes (2004), incipient drought occurs when the scPDSI falls below -0.5 . Subsequently, drought severity progresses through slight, moderate, severe, and extreme levels as the scPDSI thresholds of -1.0 , -2.0 , -3.0 , and -4.0 are crossed, respectively. A lower scPDSI value indicates more severe drought conditions. The minimum scPDSI value observed during the year will be used to evaluate the annual trend in drought severity. This metric is positively correlated with the average scPDSI over the year.

Drought frequency is a crucial metric in drought assessment, defined as the proportion of months classified as drought months relative to the total number of months in the study period. This study identifies drought occurrence using a scPDSI value of less than -0.5 as the criterion. Drought frequency is evaluated across the entire study period or annually. Increased drought frequency within a year correlates positively with drought severity, indicating a higher likelihood of severe drought occurrence with increasing frequency.

Identifying the frequent drought season is crucial for effective water resource management, as it offers valuable insights into mitigating the adverse impacts of drought. The frequent drought season can be determined by analyzing the seasons during which the scPDSI frequently falls below -0.5 . This information will serve as a vital tool for anticipating and addressing drought-related challenges.

3.5. Correlation analysis

This study employs the correlation coefficient to examine the relationship between each drought characteristic and water availability. The correlation coefficient is used to determine whether yearly and seasonal water availability trends are consistent with drought trends, which will help to understand how drought influences annual and seasonal patterns in water availability. The relationship between the drought index and the anomaly in water availability is also examined using the correlation coefficient. This analysis will assess the significance of drought-induced anomalies in water availability.

3.6. Calculation of driver contribution

The water availability is calculated as P minus ET . The variability of P and ET influences the variability of water availability. Variance is a metric used to quantify the variability of time series data. To further clarify how P and ET influence the variance in water availability, the variance of water availability (WA) is decomposed as follows (Zhang et al. 2023):

$$var(WA) = var(P) + var(-ET) + 2cov(P, -ET) \quad (2)$$

where $var(P)$ and $var(-ET)$ are the variances of P and $-ET$, respectively, and $cov(P, -ET)$ is the covariance of P and $-ET$. The contribution percentage of P and ET to WA variability is quantified as

$$CP_X = \frac{|var(X)|}{|Var(P)| + |Var(-ET)| + |2Cov(P, -ET)|} \times 100\% \quad (3)$$

where X is P or ET .

In this study, the contribution of P and ET to the variability of water availability will be analyzed at both yearly and monthly scales, reflecting the interannual and seasonal variability of water

availability, respectively. This analysis is crucial for understanding the drivers of water availability across different temporal scales.

4. Results and analysis

4.1. Relationship of water deficit and drought and aridity in the Belt and Road region

Multi-year average water availability in the Belt and Road region generally aligns with the precipitation pattern and varies with latitude and land-sea location (Figure 3a). The majority of the Belt and Road region, approximately 87%, experiences a surplus of water with positive P-ET. However, the remaining 13% suffers from water deficit, primarily in the arid and semi-arid areas of central Asia and southern Africa. In these regions, farmland, grassland, and forest cultivation rely on irrigation from rivers and groundwater, creating irrigated oases such as the Hexi Corridor and Tarim

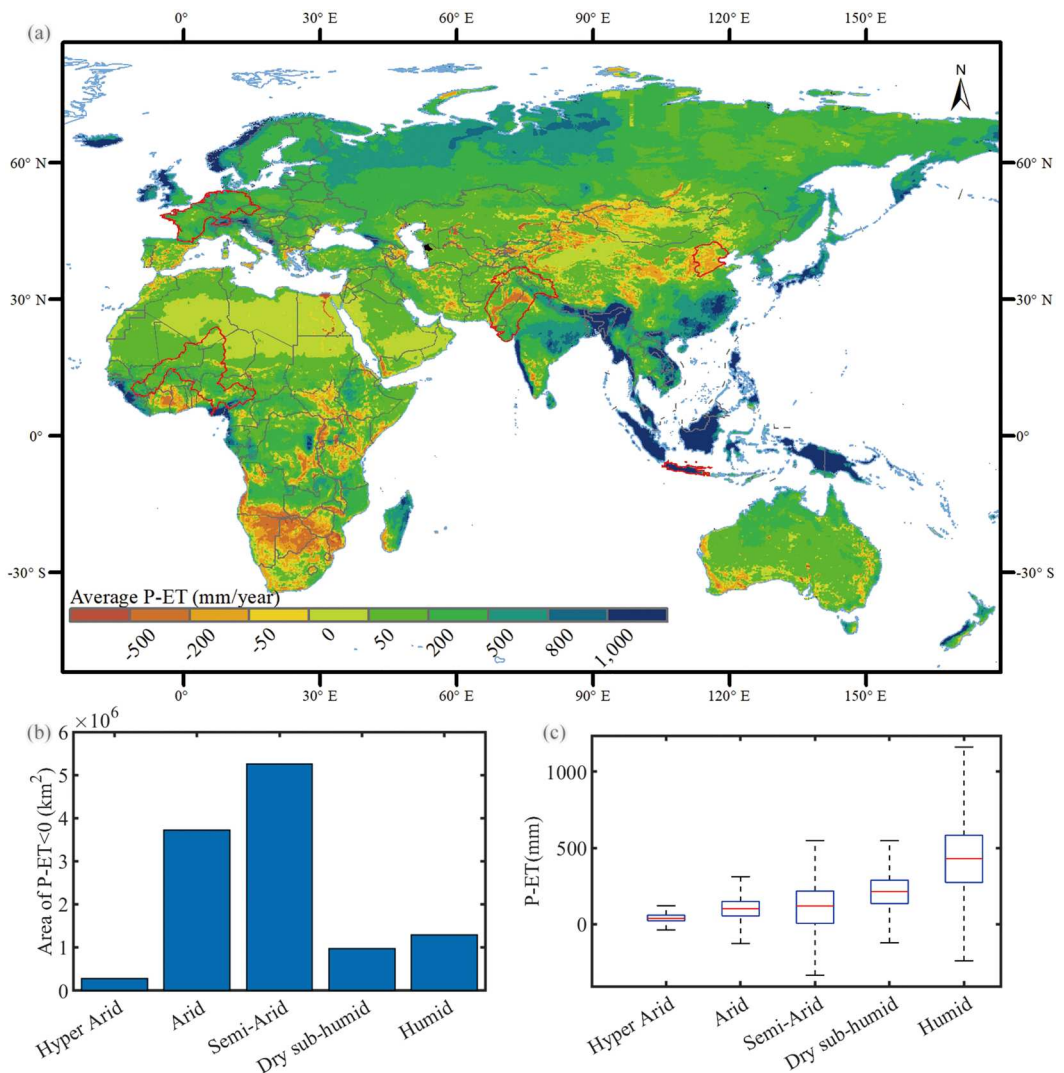


Figure 3. Spatial pattern of water availability and statistics across different climate types, (a) multi-year average P-ET pattern, (b) area with P-ET < 0, and (c) statistic distribution across climate types.

River basin in Northwestern China, the Indus River basin, and the Nile Delta. These areas typically have scarce precipitation, resulting in a significant water deficit, sometimes exceeding 500 mm/year. Meltwater from alpine mountains surrounding the oasis basins in the Northwest of China is the primary water source for evapotranspiration in these areas. Lakes and wetlands in arid and semi-arid regions, such as Central Asia, the Tibetan Plateau, Central and Eastern Africa, and the Okavango Delta in Southern Africa, also experience significant water deficits. Additionally, groundwater extraction for agricultural purposes in large irrigation areas like the North China Plain and Northwest India leads to a substantial water deficit. The significant decline in terrestrial water storage in these regions, as observed by the GRACE satellite, confirms this water deficit (Rodell and Reager 2023).

P-ET reflects the relationship between water supply and demand. $P-ET < 0$ is mainly distributed in arid and semi-arid regions due to the limited water supply and high demand (Figure 3b). $P-ET < 0$ is sporadically distributed in hyper-arid and humid areas. Hyper-arid regions have minimal water demand despite an extremely dry climate with rare precipitation, resulting in approximately negligible P-ET. Fewer regions with $P-ET < 0$ are found in humid areas because the water supply can meet most water demand. However, tremendous water consumption in humid areas can also lead to water deficits. Generally, P-ET decreases with increasing aridity (Figure 3c). The higher the aridity, the lower the water availability. The spatial variation of P-ET in semi-arid and humid regions is more significant than in the other three climate regions.

Jawa Island has the highest water availability among the five selected river basins, with more than 1000 mm/year, followed by the European rivers basin. Next in line are the Niger and Indus River Basins, with less than 200 mm/year. The Haihe River basin is in a water deficit status, meaning that water demand in this region cannot be met solely by precipitation. Numerous studies have also confirmed significant groundwater depletion for agricultural water use and increasing evapotranspiration (Zheng et al., 2022).

Drought can occur in any climate region. High drought frequency is found in Northern China, Mongolia, West Asia, Southern Africa, Australia, Central and Eastern Europe, Central Asia, and Northern India (Figure 4a). Compared with the spatial pattern of water availability in Figure 3a, there is an overlap between regions with low water availability and frequent drought areas, such as North China, Mongolia, Southern Africa, and northern India. Statistics show that water availability decreases as drought frequency increases. Low water availability is generally consistent with high drought frequency, and high water availability corresponds to low drought frequency (Figure 4b). Due to the negative relationship between drought frequency and severity, most regions with water deficits correspond to negative scPDSI values (Figure 4c), indicating drought status. Therefore, the water deficit is mainly in arid and semi-arid areas with high drought frequency.

4.2. Annual trend of water availability and the relationship with drought trend

Over the entire Belt and Road region, the average annual water availability between 2001 and 2020 was 249 mm, accounting for 35% of the annual precipitation of 707 mm. During this period, yearly water availability exhibited a decreasing trend, with fluctuations primarily following variations in precipitation (Figure 5). Precipitation contributed 67% to the variability of water availability, whereas evapotranspiration contributed only 16%. The combined contribution from precipitation and evapotranspiration was 17%. Despite an increasing trend in precipitation, the more significant increase in evapotranspiration in the Belt and Road region led to a decreasing trend in water availability. The lowest water availability occurred in 2015, mainly due to severe global droughts caused by the super-strong El Niño event. This El Niño event was one of the strongest of the 20th century, characterized by its long duration, high intensity, and high peak, which resulted in widespread regional drought and severe water stress (Anyamba et al. 2019). Conversely, La Niña events in 2007–2008, 2010–2011, and 2016–2017 brought heavy precipitation (Wang et al. 2023), leading to high water availability.

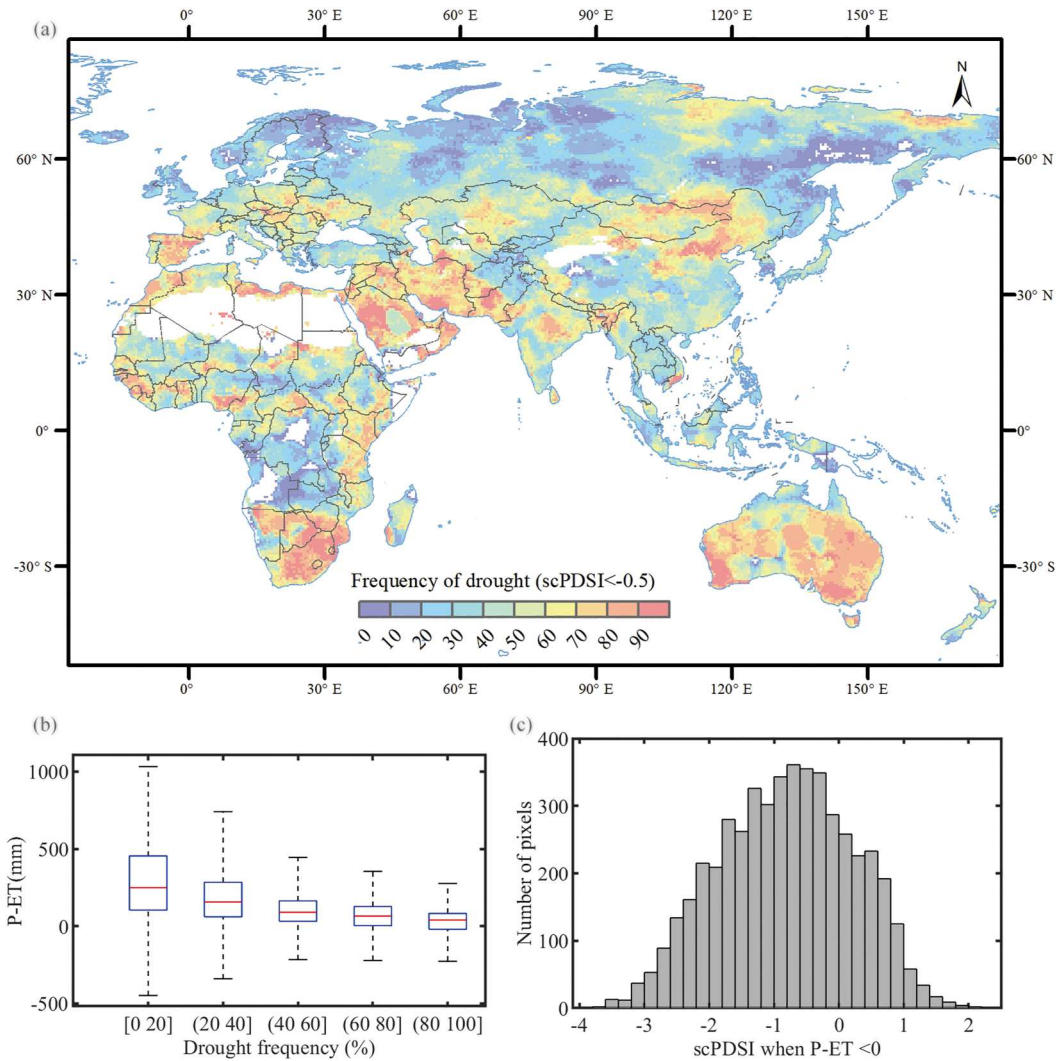


Figure 4. (a) Spatial pattern of drought frequency, (b) distribution of P-ET in different drought frequencies, and (c) the distribution of drought severity in water deficit areas.

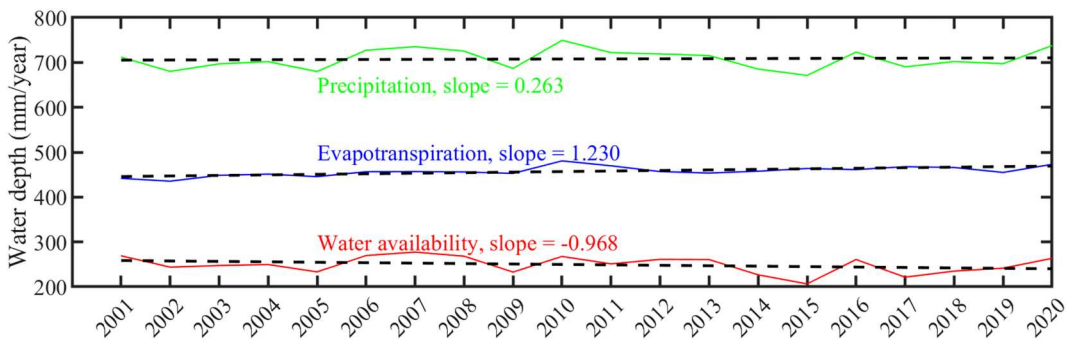


Figure 5. Annual water availability of the entire Belt and Road region from 2001 to 2020.

The annual trend of water availability in the Belt and Road region from 2001 to 2020 exhibited various spatial patterns (Figure 6a). A decrease in water availability was observed in Southeast Asia, Europe, large parts of Siberia, most of Africa, and northwestern Australia, covering 54% of the Belt and Road region. Significant declines were noted in the Indochina Peninsula, the Congo Basin, Western and Eastern Europe, and Siberia. Within those areas of decreased water availability, 8% are in water deficit regions, while 46% are in water surplus regions. The decrease in P-ET in water deficit regions indicates more severe water stress, whereas the decline in water surplus regions signifies a downgrading of water availability conditions.

Conversely, water availability increased in eastern Asia, northwestern Europe, western India, West Africa, east Africa, and eastern Australia, with significant increases in northeastern Asia, southern China, the Malay Archipelago, central and east Africa, and northwestern Russia. Regions with increased water availability accounted for 46% of the Belt and Road region, of which 5% are in

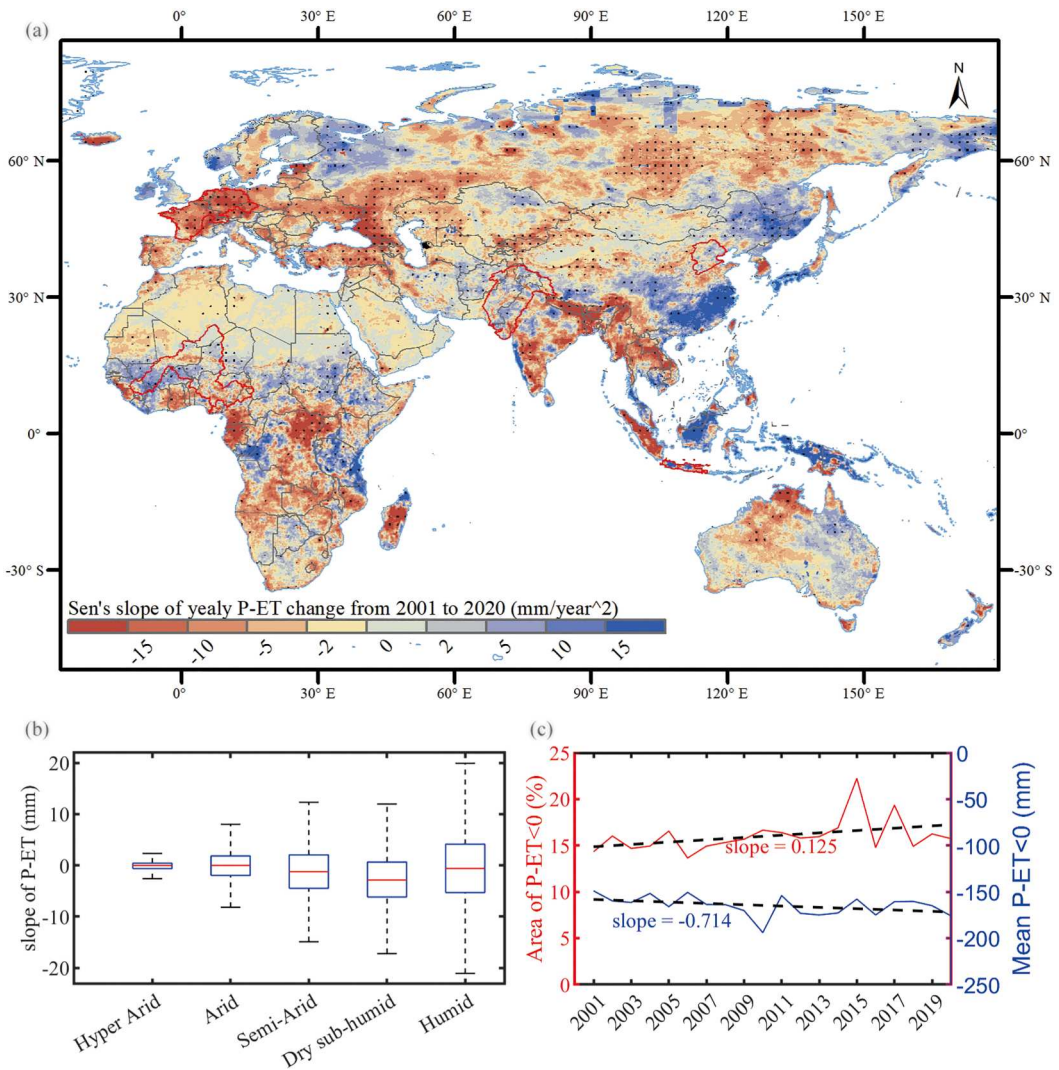


Figure 6. (a) Spatial pattern of change slope in water availability from 2001 to 2020 (The black points indicate where the trend is significant at the 0.1 significance level.), (b) the distribution of slope in different climate classes, and (c) the temporal evolution of the area percentage of water deficit and the mean water deficit.

water deficit regions and 41% are in water surplus regions. The increasing trend of P-ET in water deficit regions, such as parts of southern Africa, North Africa, and Northwest China, implies a reduction in water stress, which is a positive signal for the sustainable use of water resources. However, the increase in water availability in water surplus regions, especially in humid areas like southern China and the islands of Southeast Asia, indicates a rising flood risk. Water availability is decreasing in the arid regions and increasing in the humid areas, as found in other studies (Pang and Zhang 2023).

P-ET shows a more significant decline in the dry sub-humid region, followed by the semi-arid region (Figure 6b). Humid regions also exhibit a slight decrease in P-ET. In contrast, the change in P-ET in hyper-arid and arid areas is insignificant. The spatial variation in the P-ET trend increases as aridity decreases, becoming more pronounced in the humid areas due to higher water availability. In semi-arid climate regions, where water deficits are more prevalent, the declining trend in water availability will exacerbate the water crisis, hindering the achievement of sustainable development goals.

Over the past 20 years, from 2001 to 2020, the fractional abundance of water deficit areas in the Belt and Road region had an expanding trend (Figure 6c), indicating that water deficits are becoming more severe. The intensity of the water deficit, measured as the mean value of yearly P-ET < 0, has been gradually increasing (Figure 6c). This expanding area and the increasing intensity of the water deficit suggest that the Belt and Road region will likely encounter higher water stress and risk.

Figure 7a and b show the spatial patterns of drought frequency and severity trends, respectively. The spatial pattern of drought frequency trends is closely related to the drought severity trends, meaning that as drought frequency increases, drought severity also increases. The correlation

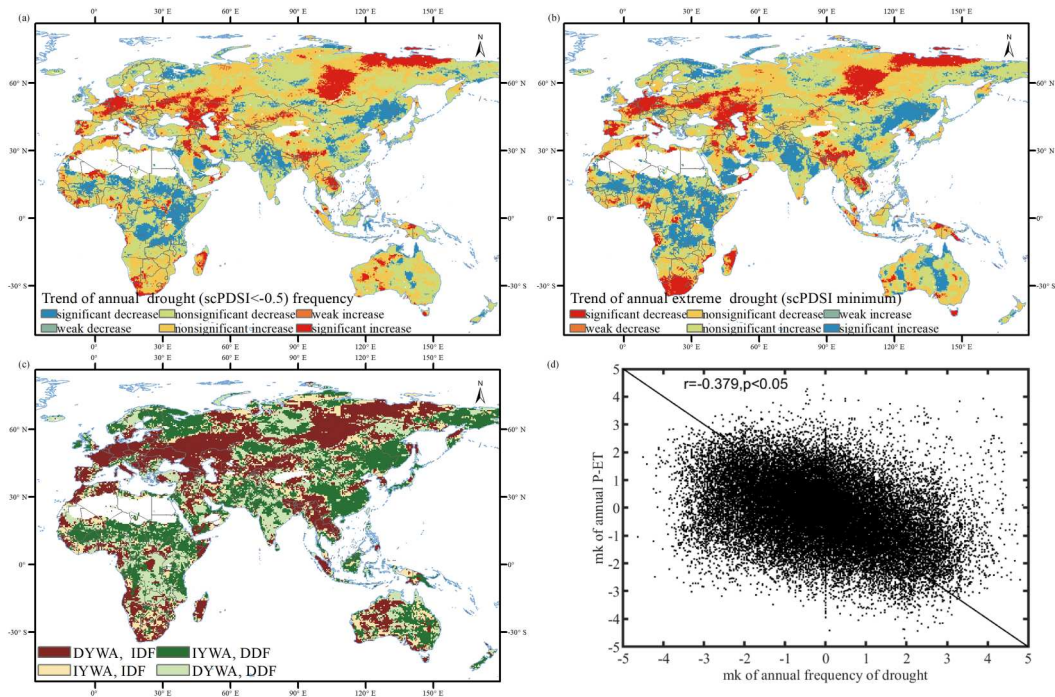


Figure 7. (a) Spatial pattern of drought frequency trend, (b) spatial pattern of drought severity trend, (c) relationship between drought frequency trend and water availability trend, and (d) scatter plot between drought frequency trend and water availability trend (DYWA: Decreased yearly water availability; IYWA: Increased yearly water availability; IDF: Increased drought frequency, and DDF: Decreased drought frequency. The legend indicating a significant decrease or increase signifies that the trend has passed the significance test at the 0.05 level, whereas a weak decrease or increase signifies that the trend has passed the significance test at the 0.1 level.)

coefficient between drought frequency and severity trends is nearly 0.9. Upon comparing these patterns with the spatial pattern of water availability trends shown in [Figure 6a](#), a clear consistency could be found between the frequency and severity of droughts and water availability trends. This consistent trend covers approximately two-thirds of the Belt and Road region ([Figure 7c](#)). Regions with significantly increased drought frequency, such as southern Europe, large parts of Siberia, Southeast Asia, southern Africa, and northwestern Australia, also exhibit decreasing water availability, accounting for 30% of the Belt and Road region.

Conversely, areas where drought frequency has significantly reduced, such as eastern Asia, northern Europe, and most of Africa, show an increase in water availability, accounting for 28% of the Belt and Road region. The scatter plot in [Figure 7d](#) further illustrates this negative relationship: increased drought frequency corresponds to decreased water availability, and reduced drought frequency corresponds to increased water availability. This high consistency is primarily due to the intrinsic similarity between the two indicators of scPDSI and P-ET, which are mainly influenced by precipitation and based on the water balance concept. Inconsistencies are mostly found in parts of central Russia, central Africa, and South Asia. These inconsistent regions can be divided into two scenarios: one where increased drought frequency occurs alongside increased P-ET and another where decreased drought frequency occurs with reduced P-ET. Apart from the inconsistent change rate of precipitation and evapotranspiration, other social and economic factors also impact water availability (Cooley, Ryan, and Smith 2021; Rachunok and Fletcher 2023).

4.3. Seasonality of water availability and the impact of drought

4.3.1. Seasonal changes in water availability and drivers

The monthly P-ET throughout the year effectively represents the seasonal variability in water availability. The standard deviation is used to quantify the seasonality of monthly time-series data. The seasonality of water availability generally follows the seasonality of precipitation spatially and is greater than the seasonality of evapotranspiration ([Figure 8a–c](#)). High seasonality of water availability is mainly found in Southeast Asia, South Asia, central Africa, and northern Australia, followed by European regions. Those regions had abundant precipitation and evapotranspiration ([Figure 2c, d](#)). Interestingly, the seasonality of water availability is greater than that of precipitation in some parts of Europe. Across the entire Belt and Road region, P-ET is higher from July to September than in other months, consistent with the distribution of precipitation ([Figure 8d](#)). However, water availability from April to June is significantly lower than in other months due to relatively low precipitation and high evapotranspiration. Low water availability during these months indicates high water stress.

The seasonal change of P-ET in five typical river basins is shown in [Figure 8e–i](#) to illustrate the seasonality of water availability. The seasonal change of P-ET in the Haihe River basin, Indus River basin, and Niger River basin generally follows the seasonal shift in precipitation, with higher P-ET and precipitation in July or August. However, a significant water deficit can be observed from March to June (spring) in the Haihe River basin ([Figure 8g](#)), primarily due to high evapotranspiration from extensive irrigation needed to ensure food security. In the Indus River basin and Niger River basin, water deficits mainly occur from October to December, indicating higher water stress during this season ([Figure 8f, h](#)). European rivers basin exhibits an opposite seasonal change, with lower water availability and even water deficits from May to July (summer) ([Figure 8e](#)). The western European river basin is mainly influenced by a temperate maritime climate characterized by evenly distributed rainfall throughout the year, with slightly heavier rainfall in winter. In contrast, a temperate continental climate primarily affects the east of the European rivers basin, with hot summers and limited precipitation. These climatic conditions lead to high summer evapotranspiration and low water availability. Java Island, located in the Southern Hemisphere, experiences different seasons compared to the Northern Hemisphere ([Figure 8i](#)). The water deficit from June to September is due to scarce precipitation during this period, while evapotranspiration remains generally high

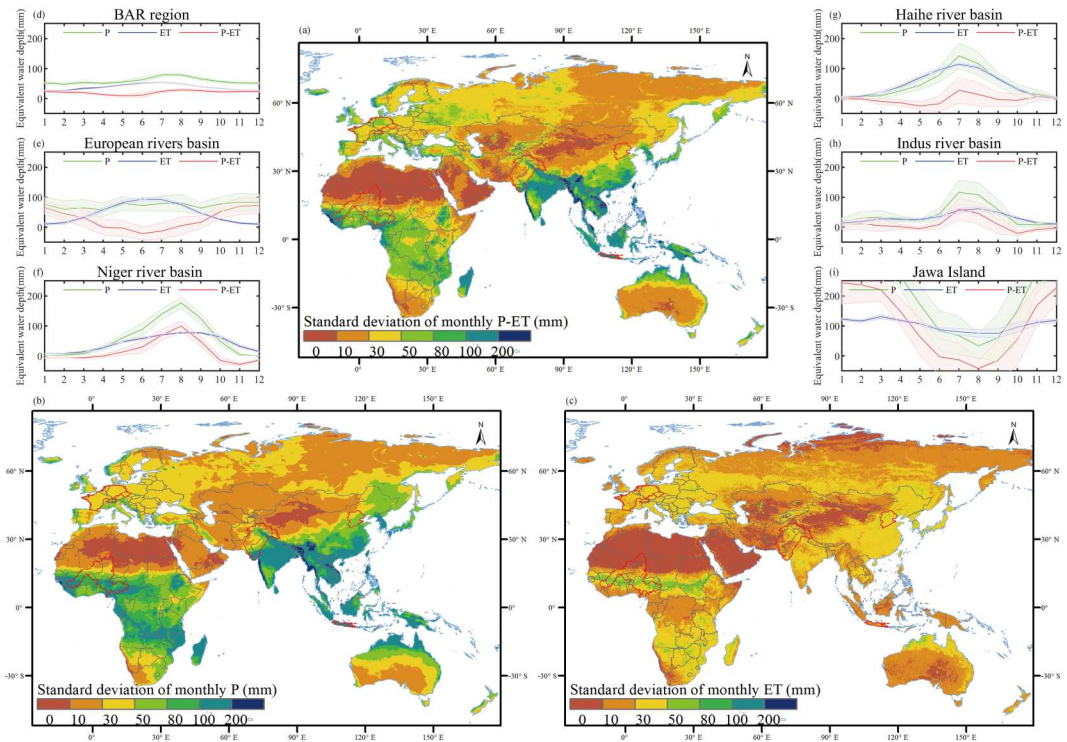


Figure 8. Seasonality of water availability and its related variables in the Belt and Road region in 2001–2020.

throughout the year, averaging about 100 mm/month. Overall, the seasonal change in water availability varies with the seasonality of precipitation, evapotranspiration, and geographical location.

Further analysis was conducted to determine the dominant factors influencing the seasonal change in water availability, calculated using equation (6). For the entire Belt and Road region, precipitation contributes 32% to the monthly variability in water availability, while ET contributes 25%. The remaining 43% of the monthly variability in P-ET is primarily due to the synergy between precipitation and evapotranspiration. This contribution differs from that on a yearly scale. The contribution of precipitation is lower at the monthly scale, while the contributions from ET and the synergy of P and ET increase with the decreasing time scale. These results indicate that the influence of precipitation and evapotranspiration on water availability varies with time scales. Specifically, the contribution of ET to the variability of water availability is higher on a monthly scale than on a yearly scale, which is also illustrated spatially (Figure 9).

Evapotranspiration significantly determines the seasonal variability of water availability in northern Eurasia (Figure 9a). Regions where the synergy of precipitation and evapotranspiration is dominant are primarily found in semi-arid areas, including north Asia, the Sahel region of North Africa, southern Africa, and Australia. These findings align with previous studies that highlight the more significant contribution of evapotranspiration to changes in land water storage at middle and high latitudes (Zhang et al. 2019) and the intensification of water availability during the dry season driven mainly by increased evapotranspiration rather than decreased precipitation (Padrón et al. 2020). Precipitation dominates the variability of yearly water availability for most of the Belt and Road region (Figure 9b). However, in arid and semi-arid areas, evapotranspiration and the combination of precipitation and evapotranspiration play more significant roles in the variability of yearly water availability. These results are consistent with the conclusions of Zhang et al. (2023). Thus, when considering the seasonal variability of water availability, it is crucial to focus

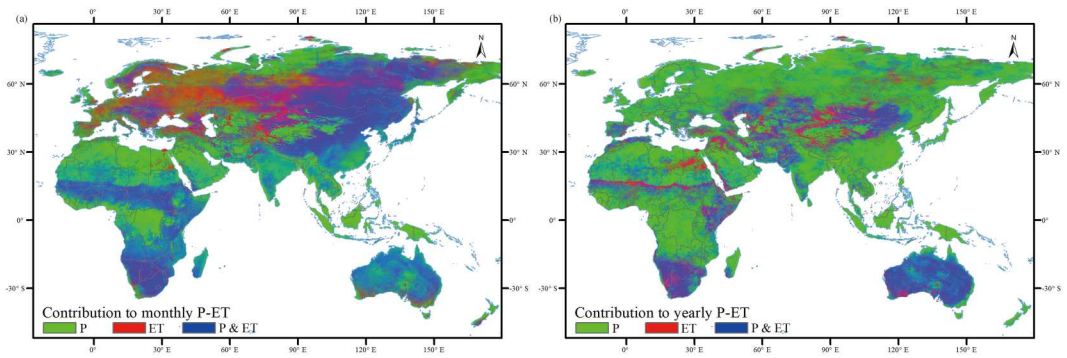


Figure 9. Contribution of precipitation and evapotranspiration to the variability of water availability, (a) at the monthly scale and (b) at the yearly scale (The figure is a composite image that uses three colors. The colors green, red, and blue represent the contributions from P, ET, and the synergy between P and ET, respectively. A color closer to green indicates a greater contribution from P, while red and blue indicate the contributions from ET and the synergy between P and ET, respectively. The different colors reflect the varying contributions of the three components.).

on the contributions of evapotranspiration and the combined effect of precipitation and evapotranspiration.

4.3.2. Relationship between low water availability seasons and frequent drought seasons

Droughts, typically accompanied by high temperatures, accelerate surface evapotranspiration and reduce available water. Droughts occurring in seasons of low water availability exacerbate water stress. Clarifying the relationship between low water availability and frequent drought seasons is crucial for sustainable water management. As shown in [Figure 10a](#), the seasons of low water availability generally vary with latitude. However, drought-prone seasons do not always align with seasons of low water availability ([Figure 10b](#)).

Approximately one-third of the Belt and Road region, particularly areas north of 30°N, experiences consistency between drought-prone seasons and minimum water availability seasons. Widespread regions of Europe and northern Asia, experiencing high evapotranspiration from June to August (summer), are also prone to droughts during this season. In the Midwest of Australia, the consistency between the drought-prone season and the low water availability season is also found from June to August, corresponding to winter in this region. Fragmented areas in the Northern Hemisphere, such as northern China, southwest China, and central Asia, have low water availability from March to May (spring) but also experience frequent droughts during this season. This

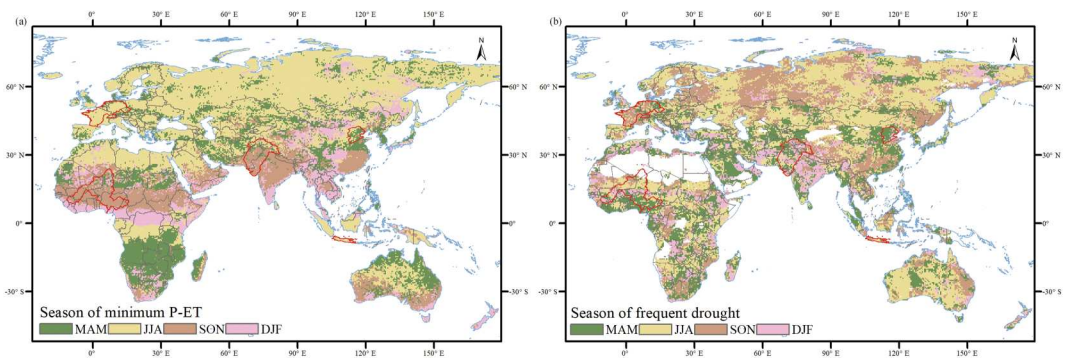


Figure 10. (a) Seasons of minimum water availability and (b) seasons of frequent drought in the Belt and Road region from 2001 to 2020.

period is crucial for agricultural production, and the overlap of low water availability and frequent droughts is detrimental to crop growth. Among the five focus basins, the Hai River Basin and Java Island experience frequent droughts during seasons of low water availability. In the other three basins, frequent droughts lag behind the seasons of low water availability.

4.3.3. Annual trend of water availability seasonality and the impact of drought

The increase in the seasonality of water availability signifies a more significant disparity between wet and dry seasons throughout the year, while the decrease means the difference between dry and wet seasons is reduced. Across the Belt and Road region, areas experiencing increases in P-ET seasonality account for 60% of the region. These areas are primarily concentrated in north-central Asia, Northern and Eastern Europe, northern and eastern Africa, and eastern Australia (Figure 11a). Conversely, decreases in P-ET seasonality are observed in 40% of the region, mainly in Central Asia, eastern Russia, North Africa, Central and Southern Africa, and western Australia. Compared to Figure 6a, the seasonality trend of water availability is positively correlated with the annual trend, indicating that regions experiencing an increase in annual water availability also tend to have an increase in seasonality and vice versa. The rise in seasonality also contributes to the overall increasing yearly trend.

Extreme drought significantly impacts the seasonality of water availability. Compared with the trend of extreme drought in Figure 7b, increased drought severity leads to heightened water availability seasonality in 20% of the Belt and Road region. These areas are primarily distributed in Siberia, central Europe, and parts of southwest China (Figure 11b), with increased summer heatwaves in Europe illustrating this well (Zhang et al. 2020). Conversely, regions where water availability seasonality decreases with decreased drought severity account for about 20% of the Belt and Road region, mainly in central Africa, parts of Europe, and central Australia. A decrease in drought severity often corresponds with increased precipitation, which may primarily occur during the season of low water availability, leading to a reduction in water availability seasonality.

Regions of increased water availability seasonality with decreased drought severity account for 35% of the Belt and Road region. Besides drought, the increase in water availability seasonality in East Asia, North and East Africa, Northern Europe, and parts of South Asia, which aligns with areas of increased annual water availability shown in Figure 6a, is also attributed to extreme precipitation. Significant increases in abrupt shifts between drought and flood events have been observed in China (Zhang et al. 2023), serving as an excellent example of this phenomenon.

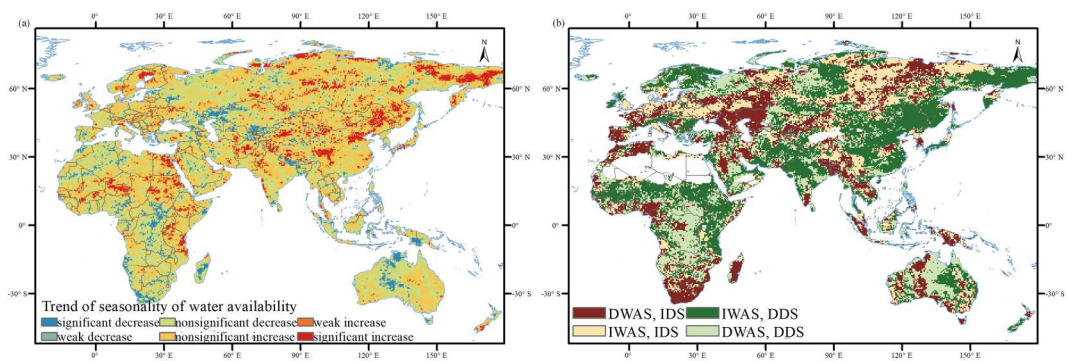


Figure 11. (a) The trend of the seasonality of water availability, and (b) the relationship with drought severity trend (DWAS: Decreased water availability seasonality; IWAS: Increased water variability seasonality; IDS: Increased drought severity; and DDS: Decreased drought severity. The legend indicating a significant decrease or increase signifies that the trend has passed the significance test at the 0.05 level, whereas a weak decrease or increase signifies that the trend has passed the significance test at the 0.1 level).

In regions where water availability seasonality decreases with increased drought severity, extreme droughts may mainly occur during seasons of high water availability. Thus, even with an increasing trend in drought severity, the seasonality of water availability may still decrease. Additionally, factors other than precipitation, such as changes in land use, water management practices, and temperature variations, may also contribute to seasonal changes in water availability (Cui et al. 2022; Guo et al. 2023; Wang et al. 2024; Zhou et al. 2022).

4.4. Comparison between drought index and P-ET anomaly

Drought events lead to a decrease in water resources. Specifically, when drought occurs, water availability decreases compared to a normal year during the same period, leading to a negative anomaly in water availability. As drought severity intensifies, the anomaly of P-ET increases negatively. The spatial distribution of the correlation between the P-ET anomaly and the scPDSI is shown in Figure 12a.

A strong positive correlation exists between P-ET anomalies and scPDSI in the northern, eastern, and southeastern parts of the Asian continent and relatively humid areas. This correlation indicates that the negative anomaly in water availability also increases as drought severity intensifies. However, this positive relationship is not consistently observed in the arid and semi-arid regions of Africa, Central Asia, West Asia, and Australia. In some of these regions, there is a slight negative correlation between P-ET anomaly and scPDSI.

The histogram in Figure 12b also shows that most negative P-ET anomalies occur under drought conditions. When there is no drought, the average P-ET anomaly is always positive. Conversely, during droughts, the average P-ET anomaly is always negative (Figure 12c). Under extreme drought conditions, the negative anomaly of P-ET is most significant.

The P-ET anomalies and the time evolution of scPDSI in five typical basins are shown in Figure 12d-h. P-ET anomalies generally follow the changes in scPDSI to a certain extent. The correlation

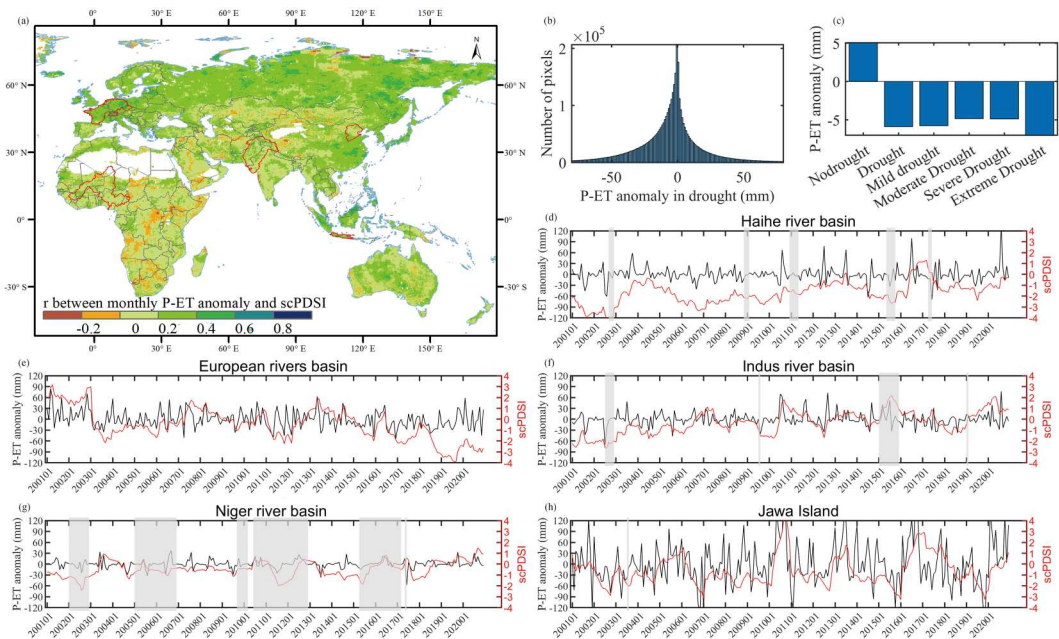


Figure 12. Relationship between monthly P-ET anomaly and scPDSI.

coefficient is higher in humid regions than in arid and semi-arid areas. The overall P-ET anomalies and scPDSI changes were consistent in European river basins. Especially before 2018, high scPDSI values corresponded to positive P-ET anomalies, and low scPDSI values corresponded to negative P-ET anomalies well. However, from 2018 to 2020, Europe experienced severe droughts and heat waves (Rakovec et al. 2022), which were well identified by the scPDSI index. However, drought and heat waves did not cause significant negative anomalies in water availability.

The Niger River basin in Africa is prone to droughts. The recorded drought events are consistent with most scPDSI index values and P-ET negative anomalies. However, some inconsistencies exist with the basin scale since the drought record is based on the provincial scale. For example, in 2016, there may have been no drought in the entire basin, while the recorded drought may refer to a drought in a specific region.

The Haihe River Basin and Indus River Basin also have frequent droughts. The drought index in these regions is not strongly correlated with the P-ET anomaly. Jawa Island, located in a tropical area, has abundant rainfall resources but also experiences droughts, which cause negative anomalies in water availability.

There are a few reasons for the inconsistency between scPDSI and the water availability anomaly. First, there may be uncertainties in the drought index in arid and semi-arid regions and uncertainties from remote sensing-based precipitation and evapotranspiration data. Second, other factors, such as human activities, affect water availability. In drought conditions, many measures, such as adapted water management policies, are implemented to mitigate the impact of drought, altering the consistent relationship between P-ET anomaly and scPDSI.

5. Discussion

5.1. Reliability of data

This study investigated the spatial and temporal characteristics of water availability in the Belt and Road region using high-resolution precipitation and evapotranspiration data. The accuracy of this data was validated during the development of the algorithms (Zheng et al., 2022). To further ensure data reliability, we compared our results with those of Zhang et al. (2023), who studied global land water availability trends from 2001 to 2020 using multi-source data. We found that the overall decrease in water availability in the Belt and Road region aligns with the global declining trend reported by Zhang et al. (2023). Since the Belt and Road region covers two-thirds of the worldwide land area (excluding Antarctica and Greenland), our results have significant global implications.

The spatial distribution of interannual changes in water availability shown in Figure 6a of this study closely matches the aggregated results from multi-source data in Figure 1B of Zhang et al. (2023), with similar regions exhibiting increasing and decreasing trends. Regions with increasing trends include northeastern Asia, southern China, northwestern Europe, western India, West Africa, southeastern Africa, and eastern Australia. Regions with decreasing trends include Southeast Asia, eastern Europe, large parts of Siberia, most of sub-Saharan Africa, and central and northwestern Australia. Furthermore, the spatial patterns shown in Figures 3a and 6a also agree with those obtained from the Multi-Source Weighted-Ensemble Precipitation (MSWEP, Beck et al. 2019) and Global Land Evaporation Amsterdam Model (GLEAM 4.1a; Miralles et al. 2024) evapotranspiration data at a coarse resolution of 10 km (Figure S1). The GLEAM ET is calculated by the water balance method using the MSWEP precipitation. These consistent findings further confirm the reliability of the data utilized in this study.

Due to the complexity of drought, many drought indices have been developed. This study used the scPDSI drought index to identify drought characteristics. We compared scPDSI with another commonly used drought index, the Standardized Precipitation-Evapotranspiration Index (SPEI). SPEI expresses the deviations of the current climatic balance (precipitation minus potential evapotranspiration) to the long-term balance, providing drought information across multi-scale

(Vicente-Serrano, Beguería, and López-Moreno 2010). The 1-month SPEI was used in this study, which is from <https://digital.csic.es/handle/10261/332007>.

The comparison between scPDSI and SPEI found that both indices are very similar across most Belt and Road regions, with most correlation coefficients larger than 0.4 (Figure 13a). For identifying drought characteristics, the correlation between the two indices was 0.639 for drought frequency identification at the 0.05 significance level (Figure 13b). The scPDSI identified drought frequencies ranging from 0% to 100%, while the SPEI identified those ranging from 20% to 80%. This discrepancy may be due to different drought classification thresholds. The average drought severity determined by the two indices was also very consistent, with an r of 0.7 (Figure 13c). For the trend of drought frequency, the correlation between the two indices was 0.637 (Figure 13d). The consistency in the seasonal drought trend was 0.539 (Figure 13e). Although the optimal time scale is not used in this study (Lu et al. 2022), the strong relationship between scPDSI and SPEI and the consistency in identifying drought characteristics further illustrate the reliability of the drought index data used in this study.

5.2. Comparison with the previous study

This study differs from previous research in several key aspects. Firstly, it utilizes high-resolution precipitation and evapotranspiration data, with a resolution of 5 km for precipitation and 1 km for evapotranspiration. These data can provide more detailed spatial patterns than previous studies, which typically had a spatial resolution of 0.5° (Allan 2023; Konapala et al. 2020; Liu et al. 2018; Padrón et al. 2020; Zhang et al. 2023). The high-resolution data better reflect P-ET in small areas like oasis regions, which helps identify the areas with water deficits.

Secondly, this study provides a spatial distribution of water availability based on the multi-year average P-ET value. It identifies regions experiencing water deficits and establishes the relationship between water deficit and drought occurrence, which is crucial for water resource management and policy-making. In the previous study, more attention is given to the trend of water availability or the special dry seasons (Allan 2023; Padrón et al. 2020; Zaitchik et al. 2023; Zhang et al. 2023; Zhao, Ma, and Wu 2021). The spatial distribution of water deficit and its change are not highlighted due to the limited rough spatial resolution data.

Thirdly, this study examines not only the interannual changes in water variability but also focuses on seasonal changes and seasonality trends in water availability. By identifying the seasons with low water availability and frequent droughts, this study highlights the regions and the periods of higher water stress.

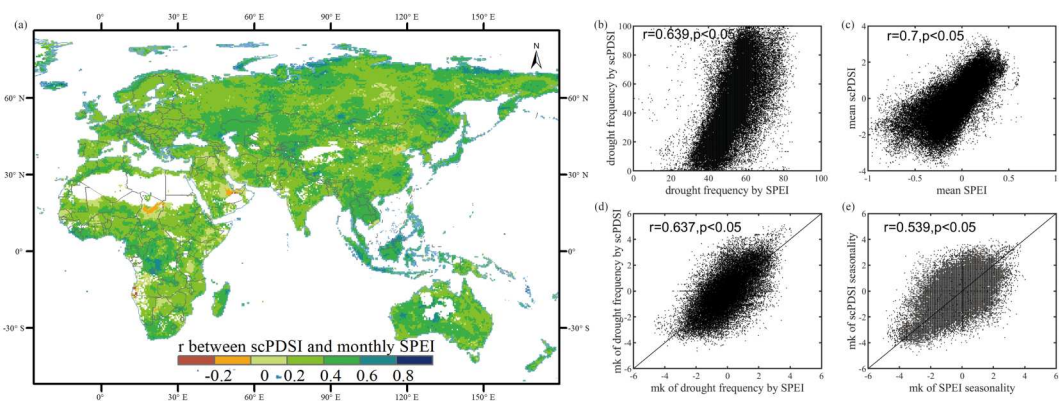


Figure 13. Relationship between scPDSI and SPEI, (a) spatial pattern, (b) drought frequency, (c) drought severity, (d) trend of drought frequency, and (e) trend of drought seasonality.

Lastly, and most importantly, the research emphasizes the relationship between drought characteristics and the temporal and spatial patterns in water availability. It also quantifies the magnitude of drought-induced anomalies in water availability. Unlike previous studies where drought and water availability were often examined separately, this study comprehensively explains the interplay between drought and water availability.

5.3. Limitations and prospects

Drought is a crucial factor influencing water availability. This study further clarifies the relationship between drought and water availability by analyzing temporal and spatial characteristics. However, the change in water availability is governed by many factors besides drought (Padrón et al. 2020; Zhao et al. 2016; Zhao, Ma, and Wu 2021). Using P-ET as a metric to characterize water availability diverges from actual renewable water resources. P-ET primarily focuses on the vertical flow of water, overlooking horizontal water transfers and utilization (Lu et al. 2019). This approach may lead to an underestimation of water availability, potentially exaggerating the impact of drought-induced water deficit. Besides, the water stress resulting from drought can be mitigated through the regional redistribution of water resources (Tabari and Willems 2023; Yan et al. 2022).

In subsection 5.1, we discussed the reliability of the data used in our study, but it is important to recognize that data uncertainties are unavoidable. The high spatial resolution precipitation data depends on TRMM-based retrieval methods and downscaling techniques, which may introduce some uncertainty. Similarly, estimating evapotranspiration using remote sensing data can be challenging due to the complexity of the land surface and potential input errors (Zheng et al., 2022). We focused our analysis on the spatial and temporal patterns of water availability rather than on specific values to minimize the influence of systematic errors in the retrieval algorithms or estimation models. Regarding the scPDSI drought index, although it has limitations in quantifying drought trends and severity in arid regions and is less sensitive to severe meteorological droughts compared to other indices (Khorrami, Ali, and Gündüz 2023; van der Schrier, Jones, and Briffa 2011; Xu et al. 2021), it has been shown to effectively identify over 80% of global drought events, including many within the Belt and Road region (Lu et al. 2022).

Water availability plays a crucial role in determining the level of water stress, which is an indispensable aspect of fostering sustainable development. According to the UN-Water (2021) definition, water stress is the ratio of total freshwater withdrawals to the available water resources within a region. The decrease in water availability directly increases water stress. Conversely, an increase in water availability can effectively alleviate water stress. The analysis of the characteristics of water availability and the relationship with droughts offers invaluable insights for evaluating the sustainable utilization of water resources.

6. Conclusion

In light of increasing water stress due to climate change, especially in water-limited regions, this study analyzed the impact of drought on the spatial and temporal characteristics of water availability using high-resolution data on precipitation and evapotranspiration. The study focused on the Belt and Road region, characterized by arid and semi-arid conditions and frequent droughts. By establishing the relationship between drought and water availability, regions with water deficits were identified, and their relationship with drought occurrence was clarified. The influence of drought on annual and seasonal trends in water availability and the exacerbation of seasonal water stress by drought were explored. Additionally, the anomalies in water availability induced by drought were quantified. Key findings are summarized as follows:

- (1) The average annual water availability in the entire Belt and Road region is 249 mm, showing a decreasing trend from 2001 to 2020, consistent with the global trend. The majority of the Belt

and Road region (87%) experiences a water surplus ($P-ET > 0$), while 13% faces water deficits ($P-ET < 0$). These deficits are mainly found in arid and semi-arid regions with high drought occurrence frequency. Furthermore, the areas and severity of water deficits are increasing in the Belt and Road region.

- (2) The annual trend of water availability is highly correlated with drought trends. Water availability decreases with increased drought frequency and vice versa. Significant decreases mainly occur in dry-subhumid and semi-arid regions. Regions experiencing an increase in annual water availability also tend to have an increase in seasonality and vice versa. The trend of drought severity in different seasons also influences the trend of water availability seasonality.
- (3) Seasonal changes in water availability are determined by precipitation and evapotranspiration. The variation in seasonality differs across regions, generally higher in the humid areas than in the arid areas. The contribution of evapotranspiration to seasonal water availability is more significant than on a yearly scale. Drought intensifies the seasonality of water availability, primarily in Siberia, central Europe, and parts of southwest China. The overlapping seasons with low water availability and drought-prone seasons, mainly in Europe and northern Asia, exacerbate seasonal water stress.
- (4) Drought leads to a negative anomaly in water availability. As drought severity intensifies, the anomaly of $P-ET$ increases negatively. There is a strong positive correlation between $P-ET$ anomalies and scPDSI in the northern, eastern, and southeastern parts of the Asian continent and relatively humid areas.

Water availability plays a crucial role in determining the level of water stress, a key indicator for sustainable development goals. Drought significantly influences water availability. Analyzing the impact of drought on water availability provides invaluable insights for evaluating the sustainable utilization of water resources. In future research, more detailed investigations will be conducted into specific sub-regions or deeper exploration of the mechanisms linking drought severity to water availability anomalies.

Disclosure statement

No potential conflict of interest was reported by the author(s).

Funding

This work was jointly funded by the National Natural Science Foundation of China [grant number: 42271394], the Open Research Program of the International Research Center of Big Data for Sustainable Development Goals [grant number: CBAS2023OPR05], and the Chinese Academy of Sciences President's International Fellowship Initiative [grant number: 2020VTA0001].

Data availability statement

The data supporting the findings of this study come from public datasets, which are described in section 3.2. Data availability is not applicable to this article as no new data were created or analyzed in this study.

Author contributions

Conceptualization and methodology: J. L., L. J., M. M.; validation, investigation, data curation, and writing – original draft preparation: J. L., C. Z., G. H., D. J.; writing – review, editing, and supervision: J. L., L. J., M. M., C. Z., G. H., D. J.; project administration: J. L., L. J., M. M.; funding acquisition: J. L. and L. J. All authors have read and agreed to the published version of the manuscript.

ORCID

Jing Lu  <http://orcid.org/0000-0003-2149-7071>
 Li Jia  <http://orcid.org/0000-0002-3108-8645>
 Massimo Menenti  <http://orcid.org/0000-0001-9176-4556>
 Chaolei Zheng  <http://orcid.org/0000-0002-6085-8274>
 Guangcheng Hu  <http://orcid.org/0000-0003-2940-8336>
 Dabin Ji  <http://orcid.org/0000-0001-6388-2555>

References

- Abbrar Faiz, M., Y. Zhang, X. Tian, J. Tian, X. Zhang, N. Ma, and S. Aryal. 2022. "Drought Index Revisited to Assess its Response to Vegetation in Different Agro-climatic Zones." *Journal of Hydrology* 614:128543. <https://doi.org/10.1016/j.jhydrol.2022.128543>.
- AghaKouchak, A., A. Farahmand, F. S. Melton, J. Teixeira, M. C. Anderson, B. D. Wardlow, and C. R. Hain. 2015. "Remote Sensing of Drought: Progress, Challenges and Opportunities." *Reviews of Geophysics* 53 (2): 452–480. <https://doi.org/10.1002/2014RG000456>.
- Allan, R. P. 2023. "Amplified Seasonal Range in Precipitation Minus Evaporation." *Environmental Research Letters* 18 (9): 094004. <https://doi.org/10.1088/1748-9326/acea36>.
- Anyamba, A., J. P. Chretien, S. Britch, et al. 2019. "Global Disease Outbreaks Associated with the 2015–2016 El Niño Event 2015–2016 El Niño Event." *Scientific Reports* 9:1930. <https://doi.org/10.1038/s41598-018-38034-z>.
- Barichivich, J., T. Osborn, I. Harris, G. van der Schrier, and P. Jones. 2021. "Monitoring Global Drought Using the Self-Calibrating Palmer Drought Severity Index [in 'State of the Climate in 2020' eds. Dunn RJH, Aldred F, Gobron N, Miller JB & Willett KM]." *Bulletin of the American Meteorological Society* 102 (8): S68–S70. <https://doi.org/10.1175/BAMS-D-21-0098.1>.
- Beck, Hylke E., Eric F. Wood, Ming Pan, Colby K. Fisher, Diego G. Miralles, Albert I. J. M. van Dijk, Tim R. McVicar, and Robert F. Adler. 2019. "MSWEP V2 Global 3-Hourly 0.1° Precipitation: Methodology and Quantitative Assessment." *Bulletin of the American Meteorological Society* 100 (3): 473–500. <https://doi.org/10.1175/BAMS-D-17-0138.1>.
- Byrne, M. P., and P. A. O'Gorman. 2015. "The Response of Precipitation Minus Evapotranspiration to Climate Warming: Why the "Wet-Get-Wetter, Dry-Get-Drier" Scaling Does Not Hold Over Land." *Journal of Climate* 28 (20): 8078–8092. <https://doi.org/10.1175/JCLI-D-15-0369.1>.
- Chen, H., and S. Wang. 2022. "Accelerated Transition between dry and wet Periods in a Warming Climate." *Geophysical Research Letters* 49:e2022GL099766. <https://doi.org/10.1029/2022GL099766>.
- Chou, C., J. C. Chiang, C. W. Lan, C. H. Chung, Y. C. Liao, and C. J. Lee. 2013. "Increase in the Range Between wet and dry Season Precipitation." *Nature Geoscience* 6 (4): 263–267. <https://doi.org/10.1038/ngeo1744>.
- Compagno, L., M. Huss, H. Zekollari, E. S. Miles, and D. Farinotti. 2022. "Future Growth and Decline of High Mountain Asia's Ice-Dammed Lakes and Associated Risk." *Communications Earth & Environment* 3:191. <https://doi.org/10.1038/s43247-022-00520-8>.
- Condon, L. E., A. L. Atchley, and R. M. Maxwell. 2020. "Evapotranspiration Depletes Groundwater Under Warming Over the Contiguous United States." *Nature Communications* 11:873. <https://doi.org/10.1038/s41467-020-14688-0>.
- Cooley, S. W., J. C. Ryan, and L. C. Smith. 2021. "Human Alteration of Global Surface Water Storage Variability." *Nature* 591 (7848): 78–81. <https://doi.org/10.1038/s41586-021-03262-3>.
- Cui, J., X. Lian, C. Huntingford, L. Gimeno, T. Wang, J. Ding, M. He, et al. 2022. "Global Water Availability Boosted by Vegetation-Driven Changes in Atmospheric Moisture Transport." *Nature Geoscience* 15 (12): 982–988. <https://doi.org/10.1038/s41561-022-01061-7>.
- Deng, H. J., and Y. N. Chen. 2017. "Influences of Recent Climate Change and Human Activities on Water Storage Variations in Central Asia." *Journal of Hydrology* 544:46–57. <https://doi.org/10.1016/j.jhydrol.2016.11.006>.
- Dewan, T. H. 2015. "Societal Impacts and Vulnerability to Floods in Bangladesh and Nepal." *Weather and Climate Extremes* 7 (3): 36–42. <https://doi.org/10.1016/j.wace.2014.11.001>.
- Dube, T., D. Seaton, C. Shoko, and C. Mbow. 2023. "Advancements in Earth Observation for Water Resources Monitoring and Management in Africa: A Comprehensive Review." *Journal of Hydrology* 623:129738. <https://doi.org/10.1016/j.jhydrol.2023.129738>.
- Giardina, F., P. Gentile, A. G. Konings, S. I. Seneviratne, and B. D. Stocker. 2023. "Diagnosing Evapotranspiration Responses to Water Deficit Across Biomes Using Deep Learning." *New Phytologist* 240 (3): 968–983. <https://doi.org/10.1111/nph.19197>.
- Gudmundsson, L., P. Greve, and S. I. Seneviratne. 2016. "The Sensitivity of Water Availability to Changes in the Aridity Index and Other Factors—A Probabilistic Analysis in the Budyko Space." *Geophysical Research Letters* 43 (13): 6985–6994. <https://doi.org/10.1002/2016GL069763>.

- Guo, H. 2018. "Steps to the Digital Silk Road." *Nature* 554 (7690): 25–27. <https://doi.org/10.1038/d41586-018-01303-y>.
- Guo, H., J. Liu, Y. Qiu, et al. 2018. "The Digital Belt and Road Program in Support of Regional Sustainability." *International Journal of Digital Earth* 11 (7): 657–669. <https://doi.org/10.1080/17538947.2018.1471790>.
- Guo, H., Y. Qiu, M. Menenti, Chen Fang, L. Zhang, J. Genderen, I. Natarajan, et al. 2017. "DBAR: International Science Program for Sustainable Development of the Belt and Road Region Using Big Earth Data." *Bulletin of Chinese Academy of Sciences* 32 (Z1): 2–9.
- Guo, Q., C. Yu, Z. Xu, Y. Yang, and X. Wang. 2023. "Impacts of Climate and Land-use Changes on Water Yields: Similarities and Differences among Typical Watersheds Distributed Throughout China." *Journal of Hydrology: Regional Studies* 45:101294. <https://doi.org/10.1016/j.ejrh.2022.101294>.
- Hajek, O. L., and A. K. Knapp. 2022. "Shifting Seasonal Patterns of Water Availability: Ecosystem Responses to an Unappreciated Dimension of Climate Change." *New Phytologist* 233 (1): 119–125. <https://doi.org/10.1111/nph.17728>.
- Han, Q., and Z. Niu. 2020. "Construction of the Long-term Global Surface Water Extent Dataset Based on Water-NDVI Spatio-temporal Parameter Set." *Remote Sensing* 12 (17): 2675. <https://doi.org/10.3390/rs12172675>.
- He, C., Z. Liu, J. Wu, X. Pan, Z. Fang, J. Li, and B. A. Bryan. 2021. "Future Global Urban Water Scarcity and Potential Solutions." *Nature Communications* 12:4667. <https://doi.org/10.1038/s41467-021-25026-3>.
- Hong, C., A. Huang, H. Hsu, et al. 2023. "Causes of 2022 Pakistan Flooding and Its Linkage with China and Europe Heatwaves." *npj Climate and Atmospheric Science* 6:163. <https://doi.org/10.1038/s41612-023-00492-2>.
- Huang, J., H. Yu, X. Guan, G. Wang, and R. Guo. 2016. "Accelerated Dryland Expansion Under Climate Change." *Nature Climate Change* 6 (2): 166–171. <https://doi.org/10.1038/nclimate2837>.
- Jia, L., M. Mancini, B. Su, J. Lu, and M. Menenti. 2017. "Monitoring Water Resources and Water Use from Earth Observation in the Belt and Road Countries." *Bulletin of Chinese Academy of Sciences* 32:62–73.
- Kang, W., F. Ni, Y. Deng, J. Xiang, Z. Yue, M. Wu, and N. Jiang. 2024. "Drought Impacts on Blue and Green Water: A Spatial and Temporal Analysis." *Ecological Indicators* 158:111319. <https://doi.org/10.1016/j.ecolind.2023.111319>.
- Khorrani, B. 2023. "Satellite-based Investigation of Water Stress at the Basin Scale: An Integrated Analysis of Downscaled GRACE Estimates and Remotely Sensed Data." *Journal of Hydroinformatics* 25 (4): 1501–1512. <https://doi.org/10.2166/hydro.2023.062>.
- Khorrani, B., S. Ali, and O. Gündüz. 2023. "An Appraisal of the Local-scale Spatio-temporal Variations of Drought Based on the Integrated GRACE/GRACE-FO Observations and Fine-resolution FLDAS Model." *Hydrological Processes* 37 (11): e15034. <https://doi.org/10.1002/hyp.15034>.
- Khorrani, B., and O. Gündüz. 2023. "Remote Sensing-based Monitoring and Evaluation of the Basin-Wise Dynamics of Terrestrial Water and Groundwater Storage Fluctuations." *Environmental Monitoring and Assessment* 195 (7): 868. <https://doi.org/10.1007/s10661-023-11480-7>.
- Konapala, G., A. K. Mishra, Y. Wada, and M. E. Mann. 2020. "Climate Change Will Affect Global Water Availability through Compounding Changes in Seasonal Precipitation and Evaporation." *Nature Communications* 11:3044. <https://doi.org/10.1038/s41467-020-16757-w>.
- Kumar, S., R. P. Allan, F. Zwiers, D. M. Lawrence, and P. A. Dirmeyer. 2015. "Revisiting Trends in Wetness and Dryness in the Presence of Internal Climate Variability and Water Limitations Over Land." *Geophysical Research Letters* 42:10867–10875. <https://doi.org/10.1002/2015GL066858>.
- Kumar, S., D. M. Lawrence, P. A. Dirmeyer, and J. Sheffield. 2014. "Less Reliable Water Availability in the 21st Century Climate Projections." *Earth's Future* 2 (3): 152–160. <https://doi.org/10.1002/2013EF000159>.
- Lehner, B., and G. Grill. 2013. "Global River Hydrography and Network Routing: Baseline Data and New Approaches to Study the World's Large River Systems." *Hydrological Processes* 27 (15): 2171–2186. <https://doi.org/10.1002/hyp.9740>.
- Li, X., Y. Zhang, N. Ma, C. Li, and J. Luan. 2021. "Contrasting Effects of Climate and LULC Change on Blue Water Resources at Varying Temporal and Spatial Scales." *Science of The Total Environment* 786:147488. <https://doi.org/10.1016/j.scitotenv.2021.147488>.
- Liu, W., W. Lim, F. Sun, D. Mitchell, H. Wang, D. Chen, I. Bethke, H. Shiogama, and E. Fischer. 2018. "Global Freshwater Availability Below Normal Conditions and Population Impact Under 1.5 and 2 °C Stabilization Scenarios." *Geophysical Research Letters* 45 (18): 9803–9813. <https://doi.org/10.1029/2018GL078789>.
- Lu, J., L. Jia, J. Zheng, and G. Hu. 2019. "Potential of Remote Sensing-Based Water Budget for the Estimation of Regional Water Resources." *Remote Sensing Technology and Application* 34 (03): 630–638. (in Chinese).
- Lu, J., L. Jia, J. Zhou, M. Jiang, Y. Zhong, and M. Menenti. 2022. "Quantification and Assessment of Global Terrestrial Water Storage Deficit Caused by Drought Using GRACE Satellite Data." *IEEE Journal of Selected Topics in Applied Earth Observations and Remote Sensing* 15:5001–5012. <https://doi.org/10.1109/JSTARS.2022.3180509>.
- Miralles, D. G., O. Bonte, A. Koppa, O. B. Villanueva, E. Tronquo, F. Zhong, H. E. Beck, et al. 2024. "GLEAM4: Global Land Evaporation Dataset at 0.1° Resolution from 1980 to Near Present." <https://doi.org/10.21203/rs.3.rs-5488631/v1>.
- Mondal, S., K. Mishra, A. Leung, and B. Cook. 2023. "Global Droughts Connected by Linkages Between Drought Hubs." *Nature Communications* 14:144. <https://doi.org/10.1038/s41467-022-35531-8>.

- Murray-Tortarolo, G., P. Friedlingstein, S. Sitch, S. I. Seneviratne, I. Fletcher, B. Mueller, P. Greve, et al. 2016. "The dry Season Intensity as a key Driver of NPP Trends." *Geophysical Research Letters* 43 (6): 2632–2639. <https://doi.org/10.1002/2016GL068240>.
- Padrón, R. S., L. Gudmundsson, B. Decharme, et al. 2020. "Observed Changes in Dry-Season Water Availability Attributed to Human-Induced Climate Change." *Nature Geoscience* 13 (7): 477–481. <https://doi.org/10.1038/s41561-020-0594-1>.
- Palmer, W. C. 1965. "Meteorological Drought." *Tech. Rep. Weather Bureau Research Paper No. 45*. Washington DC: US Department of Commerce.
- Pandžić, K., T. Likso, I. Pejić, H. Šarčević, M. Pecina, I. Šestak, D. Tomšić, and N. S. Mahović. 2022. "Application of the Self-Calibrated Palmer Drought Severity Index and Standardized Precipitation Index for Estimation of Drought Impact on Maize Grain Yield in Pannonian Part of Croatia." *Natural Hazards* 113 (2): 1237–1262. <https://doi.org/10.1007/s11069-022-05345-4>.
- Pang, J., and H. Zhang. 2023. "Global Map of a Comprehensive Drought/Flood Index and Analysis of Controlling Environmental Factors." *Natural Hazards* 116 (1): 267–293. <https://doi.org/10.1007/s11069-022-05673-5>.
- Qiu, J., Z. Shen, and H. Xie. 2023. "Drought Impacts on Hydrology and Water Quality Under Climate Change." *Science of The Total Environment* 858:159854. <https://doi.org/10.1016/j.scitotenv.2022.159854>.
- Rachunok, B., and S. Fletcher. 2023. "Socio-hydrological Drought Impacts on Urban Water Affordability." *Nature Water* 1:83–94. <https://doi.org/10.1038/s44221-022-00009-w>.
- Rakovec, O., L. Samaniego, V. Hari, Y. Markonis, V. Moravec, S. Thober, M. Hanel, and R. Kumar. 2022. "The 2018–2020 Multi-Year Drought Sets a New Benchmark in Europe 2018–2020 Multi-year Drought Sets a new Benchmark in Europe." *Earth's Future* 10 (3): e2021EF002394. <https://doi.org/10.1029/2021EF002394>.
- Rodell, M., and J. T. Reager. 2023. "Water Cycle Science Enabled by the GRACE and GRACE-FO Satellite Missions." *Nature Water* 1:47–59. <https://doi.org/10.1038/s44221-022-00005-0>.
- Rohde, M. 2023. "Floods and Droughts are Intensifying Globally." *Nature Water* 1:226–227. <https://doi.org/10.1038/s44221-023-00047-y>.
- Schlaepfer, D., J. Bradford, W. Lauenroth, S. M. Munson, B. Tietjen, S. A. Hall, S. D. Wilson, et al. 2017. "Climate Change Reduces Extent of Temperate Drylands and Intensifies Drought in Deep Soils." *Nature Communications* 8:14196. <https://doi.org/10.1038/ncomms14196>.
- Sen, P. K. 1968. "Estimates of the Regression Coefficient Based on Kendall's tau." *Journal of the American Statistical Association* 63 (324): 1379–1389. <https://doi.org/10.1080/01621459.1968.10480934>.
- Sjöstrand, K. 2023. "Water for Sustainable Development." *Nature Water* 1:568–572. <https://doi.org/10.1038/s44221-023-00108-2>.
- Tabari, H., and P. Willems. 2023. "Sustainable Development Substantially Reduces the Risk of Future Drought Impacts." *Communications Earth & Environment* 4:180. <https://doi.org/10.1038/s43247-023-00840-3>.
- UN. 2023. "Belt and Road Initiative Crucial in Supercharging Implementation of Sustainable Development Goals, Delivering Hope to World, Secretary-General Tells Forum." Accessed February 9, 2024. <https://press.un.org/en/2023/sgsm21993.doc.htm>.
- UNESCO. 2021. *UN World Water Development Report 2021: Valuing Water*. Paris, France: UNESCO.
- UN-Water. 2021. "Progress on Level of Water Stress – Global Status and Acceleration Needs for SDG Indicator 6.4.2. Report." Accessed March 15, 2024. <https://www.unwater.org/publications/progress-level-water-stress-2021-update>.
- van der Schrier, G., J. Barichivich, K. R. Briffa, and P. D. Jones. 2013. "A scPDSI-based Global Data set of dry and wet Spells for 1901–2009." *Journal of Geophysical Research: Atmospheres* 118 (10): 4025–4048. <https://doi.org/10.1002/jgrd.50355>.
- van der Schrier, G., P. D. Jones, and K. R. Briffa. 2011. "The Sensitivity of the PDSI to the Thornthwaite and Penman-Monteith Parameterizations for Potential Evapotranspiration." *Journal of Geophysical Research* 116 (D3): D03106. <https://doi.org/10.1029/2010JD015001>.
- Venkatappa, Manjunatha, Nophea Sasaki, Phoumin Han, and Issei Abe. 2021. "Impacts of Droughts and Floods on Croplands and Crop Production in Southeast Asia – an Application of Google Earth Engine." *Science of The Total Environment* 795:148829. <https://doi.org/10.1016/j.scitotenv.2021.148829>.
- Vicente-Serrano, S. M., S. Begueria, and J. I. López-Moreno. 2010. "A Multiscalar Drought Index Sensitive to Global Warming: The Standardized Precipitation Evapotranspiration Index." *Journal of Climate* 23 (7): 1696–1718. <https://doi.org/10.1175/2009JCLI2909.1>.
- Wang, H., J. Liu, M. Klaar, A. Chen, L. Gudmundsson, and J. Holden. 2024. "Anthropogenic Climate Change has Influenced Global River Flow Seasonality." *Science* 383 (6686): 1009–1014. <https://doi.org/10.1126/science.adi9501>.
- Wang, B., W. Sun, C. Jin, X. Luo, Y. M. Yang, T. Li, B. Xiang, et al. 2023. "Understanding the Recent Increase in Multi-year La Niñas." *Nature Climate Change* 13 (10): 1075–1081. <https://doi.org/10.1038/s41558-023-01801-6>.
- Wasko, C., R. Nathan, and M. C. Peel. 2020. "Trends in Global Flood and Streamflow Timing Based on Local Water Year." *Water Resources Research* 56:e2020WR027233. <https://doi.org/10.1029/2020WR027233>.

- Wells, N., S. Goddard, and M. J. Hayes. 2004. "A Self-Calibrating Palmer Drought Severity Index." *Journal of Climate* 17 (12): 2335–2351.
- WMO. 2022. *State of Global Water Resources 2021*. Geneva, Switzerland: WMO.
- Xu, H. J., X. P. Wang, C. Y. Zhao, S. Y. Shan, and J. Guo. 2021. "Seasonal and Aridity Influences on the Relationships Between Drought Indices and Hydrological Variables Over China." *Weather and Climate Extremes* 34:100393. <https://doi.org/10.1016/j.wace.2021.100393>.
- Yan, N., B. Wu, W. Zhu, Z. Ma, X. Zhang, and D. Bulgan. 2022. "The Evolution of Irrigation Effects on Agricultural Drought Mitigation in North China." *Remote Sensing* 14 (5197). <https://doi.org/10.3390/rs14205197>.
- Yuan, X., Y. Wang, P. Ji, P. Wu, J. Sheffield, and J. A. Otkin. 2023. "A Global Transition to Flash Droughts Under Climate Change." *Science* 380: 187–191. <http://doi.org/10.1126/science.abn6301>.
- Zaitchik, B. F., M. Rodell, M. Biasutti, and S. I. Seneviratne. 2023. "Wetting and Drying Trends Under Climate Change." *Nature Water* 1:502–513. <https://doi.org/10.1038/s44221-023-00073-w>.
- Zhang, Y., B. He, L. Guo, J. Liu, and X. Xie. 2019. "The Relative Contributions of Precipitation, Evapotranspiration, and Runoff to Terrestrial Water Storage Changes Across 168 River Basins." *Journal of Hydrology* 579:124194. <https://doi.org/10.1016/j.jhydrol.2019.124194>.
- Zhang, Y., C. Li, F. H. S. Chiew, D. A. Post, X. Zhang, N. Ma, J. Tian, et al. 2023. "Southern Hemisphere Dominates Recent Decline in Global Water Availability." *Science* 382 (6670): 579–584. <https://doi.org/10.1126/science.adh0716>.
- Zhang, R., C. Sun, J. Zhu, R. Zhang, and W. Li. 2020. "Increased European Heat Waves in Recent Decades in Response to Shrinking Arctic sea ice and Eurasian Snow Cover." *npj Climate and Atmospheric Science* 3:7. <https://doi.org/10.1038/s41612-020-0110-8>.
- Zhang, D., L. Wu, X. Niu, Z. Guo, Z. Zhang, S. Li, G. Zhang, F. Ahmad, Z. Shang, and H. Xu. 2022. "Looking for Ecological Sustainability: A Dynamic Evaluation and Prediction on the Ecological Environment of the Belt and Road Region." *Sustainable Production and Consumption* 32:851–862. <https://doi.org/10.1016/j.spc.2022.06.007>.
- Zhang, Y., Q. You, S. Ullah, C. Chen, L. Shen, and Z. Liu. 2023. "Substantial Increase in Abrupt Shifts between Drought and Flood Events in China Based on Observations and Model Simulations." *Science of The Total Environment* 876:162822. <https://doi.org/10.1016/j.scitotenv.2023.162822>.
- Zhao, M., A. Geruo, Y. Liu, and A. G. Konings. 2022. "Evapotranspiration Frequently Increases During Droughts." *Nature Climate Change* 12 (11): 1024–1030. <https://doi.org/10.1038/s41558-022-01505-3>.
- Zhao, F., S. Ma, and Y. Wu. 2021. "Changes in Dry-season Water Availability and Attributions in the Yellow River Basin, China." *Frontiers in Environmental Science* 9:762137. <https://doi.org/10.3389/fenvs.2021.762137>.
- Zhao, A., X. Zhu, X. Liu, Y. Pan, and D. Zuo. 2016. "Impacts of Land use Change and Climate Variability on Green and Blue Water Resources in the Weihe River Basin of Northwest China." *CATENA* 137:318–327. <https://doi.org/10.1016/j.catena.2015.09.018>.
- Zheng, C., L. Jia, and G. Hu. 2022. "Global Land Surface Evapotranspiration Monitoring by Etmontor Model Driven by Multi-Source Satellite Earth Observations." *Journal of Hydrology* 613:128444. <https://doi.org/10.1016/j.jhydrol.2022.128444>.
- Zheng, C., L. Jia, and T. Zhao. 2023. "A 21-Year Dataset (2000–2020) of Gap-free Global Daily Surface Soil Moisture at 1-km Grid Resolution." *Scientific Data* 10:139. <https://doi.org/10.1038/s41597-023-01991-w>.
- Zheng, Z., L. Ning, D. Dai, L. Chen, Y. Wang, Z. Ma, Z. L. Yang, and C. J. P. Zhan. 2022. "Water Budget Variation, Groundwater Depletion, and Water Resource Vulnerability in the Haihe River Basin During the new Millennium." *Physics and Chemistry of the Earth, Parts A/B/C* 126:103141. <https://doi.org/10.1016/j.pce.2022.103141>.
- Zhou, S., A. P. Williams, B. R. Lintner, A. M. Berg, Y. Zhang, T. F. Keenan, B. I. Cook, S. Hagemann, S. I. Seneviratne, and P. Gentile. 2021. "Soil Moisture-Atmosphere Feedbacks Mitigate Declining Water Availability in Drylands." *Nature Climate Change* 11 (1): 38–44. <https://doi.org/10.1038/s41558-020-00945-z>.
- Zhou, S., A. P. Williams, B. R. Lintner, K. L. Findell, T. F. Keenan, Y. Zhang, and P. Gentile. 2022. "Diminishing Seasonality of Subtropical Water Availability in a Warmer World Dominated by Soil Moisture-Atmosphere Feedbacks." *Nature Communications* 13: 5756. <https://doi.org/10.1038/s41467-022-33473-9>.
- Zomer, R. J., J. Xu, and A. Trabucco. 2022. "Version 3 of the Global Aridity Index and Potential Evapotranspiration Database." *Scientific Data* 9:409. <https://doi.org/10.1038/s41597-022-01493-1>